CNRS
Centre National de la Recherche Scientifique

INFN
Instituto Nazionale di Fisica Nucleare

Virgo calibration during VSR3

L. Rolland

VIR-0610A-10

November 10, 2010

VIRGO * A joint CNRS-INFN Project
Project office: Traversa H di via Macerata - I-56021 S. Stefano a Macerata, Cascina (PI)
Secretariat: Telephone (39) 50 752 521 – Fax (39) 50 752 550 – e-mail virgo@pisa.infn.it

Contents

1 Introduction

In this note, the final parameterizations of the dark fringe sensing and of the mirror actuation for the run VSR3[1] are given. The analyzed data include the pre- and post-VSR3 calibration campaign (July and October 2010) as well as the VSR3 calibration monitoring data. The calibration period is from GPS 961000000 to 972000000. The version v2r3p10 of the module Cali has been used. The calibration methods are the same as the ones used for VSR2 [1, 5, 4]. The transfer functions formula are given in the appendix of the note [5].

The modifications of the interferometer (ITF) configuration related to calibration between the end of VSR2 (January 2010) and the start of VSR3 were summarized in the note [2]. The

[1] GPS 965595615 to 971557215

preliminary parameterizations used online during VSR3 had been measured using the pre-VSR3 calibration data in July 2010 and were also given in the note [2]. One additionnal modification were the gains of the mirror actuation in LN1 mode, increased by a factor 1.33 end of July 2010, that was not seen in the preliminary calibration measurements. This factor was updated in the online processes on September 3rd 2010 (see logbook entry 27701).

In section 1, the parameterization of the dark fringe sensing is given for completeness. The stability of the timing during VSR3 is checked. The measurements to extract the mirror and marionette actuation parameterizations respectively are shown in sections 2 and 3. In section 4, the final parameterizations are compared to the ones used online for the hardware injections of fake gravitationnal wave signals in the ITF.

2 Dark fringe sensing

The modifications applied to the timing between VSR2 and VSR3 are summarized in the note [2]. They have been done such that their effects on the channels sampled at 20 kHz cancel out. This was confirmed by measurements described in [2]: the timing parameterization is thus the same as during VSR2 [5].

It has been checked that the timing of the ADC reading the dark fringe was stable during VSR3: as shown figure 2, the delay between the start of the frame and the 1 PPS ramp from the GPS receiver, sampled by the dark fringe ADC, has been constant within 0.1 μs during VSR3.

The models of the sensing are reminded in table 1 such that all the calibration parameterizations are included in this note. The shape of the digital 8th order Butterworth filter used in the ADC of dark fringe readout at 20 kHz is shown in the figure 1.

2.1 Tables

Parameters	Full model ($f < 20\,\mathrm{kHz}$)	Simple model ($f < 2\,\mathrm{kHz}$)
Gain	1	1
Φ_0 (rad)	0	0
Delay (μs)	-59.7	49.3
Butterworth frequency (Hz)	7503.65	–

Table 1: ***Models for the sensing of the*** $Pr\_B1\_\{d2, d3, d4, d5\}$***,*** Pr_B1 ***and*** $Pr\_B1p\_\{d1, d2\}$ ***channels at 20 kHz.*** *The delays are given related to the absolute GPS time.* **Simple model***: the delay has been measured with the ramped 1 PPS. It is valid up to 2 kHz.* **Full model***: the delay is the simple model delay subtracted for the Butterworth equivalent delay. It is valid up to 20 kHz. Systematic errors are* ± 4 μs *on the delay.*

2.2 Figures

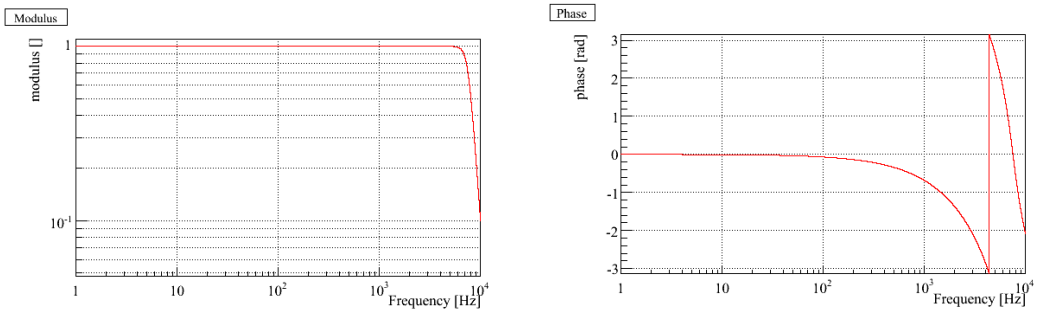

(a) TF: modulus (b) TF: phase

Figure 1: ***Model of the ADC board digital anti-alias filter of the dark fringe channel*** *sampled at 20 kHz: 8th order Butterworth filter with cut-off frequency at* 7503.65 *Hz.*

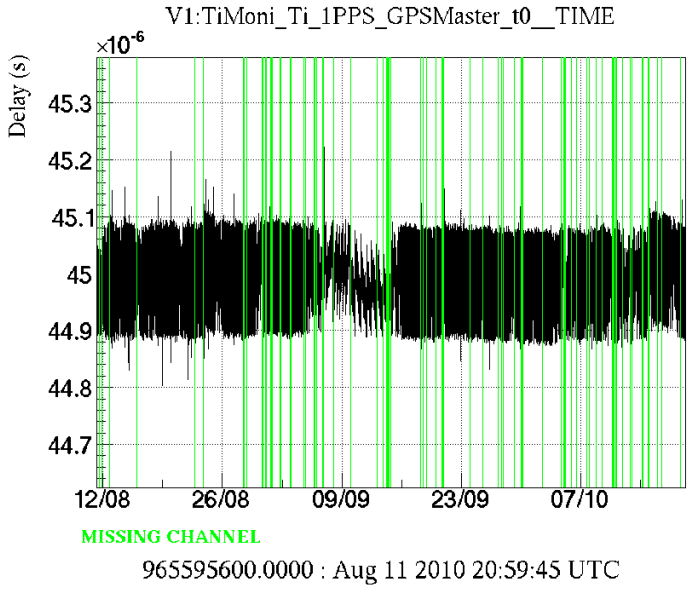

Figure 2: ***Monitoring of the delay of the dark fringe readout with respect to GPS time during VSR3*** *(not only Science Mode data).*

3 Calibration of the mirror actuation

The mirror actuation is defined as the TF (with modulus in m/V) from the correction signal sample in the Virgo DAQ to the induced mirror motion using the GPS time as reference.

In the plots that are shown, the part from the mechanical model of the pendulum has been removed. The model is defined as a 2nd order low-pass filters with $f_0 = 0.6\,\mathrm{Hz}$ and $Q = 1000$.

The mirror motion used as reference is **the effective motion on the arm differential length.** It means that the induced BS mirror motion perpendicular to its axis is $\sqrt{2}$ lower than what is measured and given in this note.

More plots are available on the web, from http://wwwcascina.virgo.infn.it/DataAnalysis/Calibration/Plots/index.html.

3.1 Description of the measurements for BS, NE and WE

The description of the data configutation and their analysis can be found in the note [5].

The first step consists in measuring the mirror actuation in High Power (HP) mode using free swinging Michelson data: the differential arm length ΔL(m) is reconstructed from the data and the transfer function (TF)[2] of ΔL over the injected noise (V) is computed to get the actuation transfer function in m/V (in the following plots, the mechanical response of the pendulum has been removed for better visibility).

The method to reconstruct ΔL has been improved compared to the one used during VSR2. The improvements were described in note [2].

Before and during VSR3, about 15 lines have been injected between 6 Hz and 1.5 kHz. During VSR3, they have been injected every two weeks with fixed amplitudes in order to monitor the stability of the actuation response. After VSR3, additionnal lines were injected in order to better constrain the parameterizations. Different amplitudes were also injected to check the linearity of the actuation response.

The second step consists in measuring the LN1/HP actuation ratio comparing in both modes the current flowing in the coil as function of the injected noise[3]. Two types of measurements have been done: (i) injection of lines at the same frequencies as the free Michelson line injection

[2] The TFs are computed using FFT lenght of 13 s for datasets shorter than 200 s. For longer datasets of d s, the FFT length is $d/10$. Only the points with coherence higher than 80% have been used.

[3] A FFT length of 4 s was used to compute the TFs. Only points with coherence larger than 99% and 99.999% were used for white noise and line injections respectively.

and (ii) injection of white noise from a few Hz to a few kHz. The line injections allow to have precise measurements at the frequencies where the actuation is known in HP mode. The white noise injections are used to check the behaviour of the ratio at all frequencies. After VSR3, the excitation has been injected with different amplitudes to check the TF linearity.
The gain of the NE and WE mirror actuation in LN1 mode has been increased by a factor 1.33 around July 21st 2010. This factor has been added in the analysis of the pre-VSR3 measurements performed earlier in July.

As a final step, the mirror actuation in LN1 mode is computed multiplying the mirror actuation in HP mode by the LN1/HP ratio. The multiplication is done using the data points measured at the free Michelson line frequencies. The data are then fitted by a model including poles and zeros.

As for the actuation in HP mode, the plots of A are not corrected for some delays. Both the "raw delay" (only corrected for the light propagation time) and the corrected delay are given in the tables with the model parameters.

Level of excitations - In case of non-linearities, it is important that the excitation levels used during the different measurements are similar. The excitation level has been estimated from the peak-to-peak amplitude of the channels that monitor the load of the coils, e.g. Ca_WE_RM_CoilU.

- HP mode: the amplitude of the channels are of the order of 10 V during the free swinging Michelson data and of the order of 2 V during the LN1 to HP ratio meauruements,
- LN1 mode: the amplitude of the channels are of the order of 0.012 V during the LN1 to HP measurements, similar to the level during Science Mode data (see figure 4).

From this criteria, the excitations in the different datasets are of the same order of magnitude. However, note that the power spectrum of the excitations are different (lines in free Michelson data, wide-band excitation for LN1/HP data and wide-band controls dominated by low-frequency ($< 100\,\mathrm{Hz}$) during Science Mode data).

3.2 Actuation calibration of BS, NE and WE mirrors

The parameters of the parameterizations fitted on the mirror actuation measurements are given in the table 3 for the configurations used in the longitudinal controls and in the table 4 for the configurations used for the hardware injections.

The figures of the different data and fit are shown in the section 3.5.

3.2.1 Actuation in HP mode

Free swinging Michelson data were analyzed to extract the actuation response A in HP mode. Statistical errors are below 1%/10 mrad in modulus and phase respectively for the frequencies

that were monitored during VSR3. They are slightly higher for the additionnal frequencies of the post-run measurements.

Time stability and linearity - The results were checked for time variability during VSR3 and for linearity, injecting excitation amplitudes within a factor ~ 2. The modulus and the phase are compatible with constants within statistics (see for example figure 5) and systematic errors are thus considered as negligible.

3.2.2 LN1 to HP TF ratio

Statistical errors are of the order of 0.3%/3 mrad in modulus and phase respectively, from 5 Hz to a few kHz.

Time stability of the ratio - The measurements during VSR3 were done with the same configurations every week, in particular the same injected noise. It allows to check the time stability of the LN1 to HP ratio. The ratio as function of time is shown at some frequencies for all the coils (for example, see figure 11). No variations are observed within the statistical error.

Linearity of the ratio - In order to check the linearity of the LN1/HP measurements, different levels of excitations have been injected within one order of magnitude during post-run measurements. The modulus and phase as function of the amplitude of the load on the coil in LowNoise1 mode are shown at some frequencies for all the coils (see for example the figure 12).

Variations are observed that are larger than the statistical errors. At 1 kHz, the phase of LN1/HP ratio tends to be ~ 20 mrad lower when the excitation level is stronger[4]. No effect is visible below 500 Hz. The phase systematic errors are thus estimated to be lower than 3 μs. In modulus, systematics are in general lower than 2%, however non-linearities are stronger for the following coils:

- **WE, coil up**: the modulus ratio differs by up to 3% between different amplitudes. No effect on the phase. (see figures 12 and 19(b)).
- **WE, coil right**: similar (see figures 18 and 20(d)).
- **NE, coil right**: similar (see figures 24 and 26(d)).
- **BS, coil down-left**: the modulus ratio decreases by up to 10% when the amplitude of the injected increases by a factor of 16. (see figures 28 and 32(b)). No effect is seen on the phase. Note that this coil has some noise issues in HP mode, coming from the DAC or the coil driver: see logbook entry 25006. Non-linearity coming from LN1 section.

[4] This effect is not seen on NE coils.

- **BS, coil up-left**: the modulus ratio differs by up to 6% between different amplitudes (see figures 27 and 31). No effect on the phase. The measurements are noiser than for the other coils. Non-linearity coming from HP section.

In order to compute the actuation response in LN1 mode, an average of the LN1/HP ratio of the corresponding coils is calculated: the effect of the non-linearities of theses three coils are thus reduced (by a factor 2 for the end mirrors and a factor 4 for BS). A systematic error of 3% on the modulus is thought to be conservative.

Note that the current sensing channel $Ca\_BS\_RM\_CoilDR$ of **coil down-right of BS** has been found to be noisy (see logbook entries 24860 and 25006). It provoks less good measuremeents of the LN1/HP ratio for this coil below a few 100's Hz as can be seen in the figure 32(d).

Differences between coils - For a given mirror, the LN1/HP ratio is different for the different coils. This might induce systematic errors since their average is used when computing the WE actuation in LN1 mode from the actuation in HP mode. The differences are of the order of 1% to 2% in modulus: the possible systematic errors that it could induce should be lower than 1%. The differences concerning the phase looks negligible (lower than 10 mrad at 1 kHz).

3.2.3 Mirror actuation in LN1 mode

The measurements of mirror actuation in LN1 mode along with the fits and the residuals are shown in figures 33 to 37. The parameterizations are given in the tables 3 and 4. The number of parameters in the fit were choosen such that the parameterization matches the data within statistics.

The measured delay are corrected for the delay induced by the simple model of the dark fringe sensing. This model has timing systematic errors of the order of 4 μs in absolute timing and 1 μs in the Butterworth filter model (assumed to be a pure delay).

Cross-check of BS mirror actuation in LN1 mode – The standard way to measure the mirror actuation in LN1 mode is done as a combination of measuremnts of the actuation in HP mode and measurement of the LN1/HP ratio. In order to cross-check the results, a direct measurement of the BS mirror actuation in LN1 mode has been performed using free swinging Michelson data. Due to limited dynamic of induced mirror motion in LN1 mode, only some frequencies have been measured, with poor statistical errors. The result is shown in the figure 38. The measurements agree with the standard ones, within the large statistical errors. Hence, no systematic errors can be highlighted.

Comparison between new and previous actuation parameterizations – The new parameterizations (in LN1 mode) have been compared to the preliminary ones (from note [2], corrected by a factor 1.33) in figure 39.

For the end mirrors and the BS mirror, both models agree within better than 0.5% in modulus and than 2 μs in phase/timing up to 1 kHz.

3.3 Calibration of the PR mirror actuation

The PR mirror actuation cannot be calibrated using free swinging Michelson data. It is calibrated comparing its response to the BS mirror actuation in HP mode. The ITF configuration for such measurements (locked cavity PR-BS-WI) is described in the note [4]: the ratio of the actuations of PR and BS is measured. The PR mirror actuation is then derived from the BS mirror actuation (in HP mode).

The ratio has been measured after VSR3 between 1 Hz and 300 Hz. Different level of excitations (white noise and lines) were applied: no non-linearity has been found. The averaged ratio is shown figure 40, with statistical errors of the order of $5-10\%$. It has been multiplied by the measured actuation TF of the BS mirror (using the measured points): the measured response of the PR mirror actuation is given in the figure 41. The fit has been performed between 1 Hz and 300 Hz and matches the data within statistics. The parameterization is given in the table 5.

3.4 Tables

Parameter	Values	Names of real pulsations
7 zeros (rad/s)	-268.962	z_1
	$-\mathrm{j}\times 53346.9$ and $+\mathrm{j}\times 53346.9$	z_2
	$-\mathrm{j}\times 65336.3$ and $+\mathrm{j}\times 65336.3$	z_3
	$-\mathrm{j}\times 117520$ and $+\mathrm{j}\times 117250$	z_4
8 poles (rad/s)	-31423.2	p_1
	$-21492-\mathrm{j}\times 10099.1$ and $-21492+\mathrm{j}\times 10099.1$	p_2, p_3
	$-13768-\mathrm{j}\times 19533.1$ and $-13768+\mathrm{j}\times 19533.1$	p_4, p_5
	$-4416.78-\mathrm{j}\times 22931.4$ and $-4416.78+\mathrm{j}\times 22931.4$	p_6, p_7
	-266.764	p_8

Table 2: ***Model of the 8th order anti-alias filter of the DAC between the DSP and the coil driver****. The full expression of the associated TF is given in appendix B.6 of note [2].*

		WE, U-D coils	NE, U-D coils	BS, four coils
LN1	Gain (μm/V)	19.885 ± 0.013	22.48 ± 0.016	89.628 ± 0.057
	Raw delay (μs)	(424.4 ± 1.1)	(420.5 ± 0.82)	(374.8 ± 1.6)
	Delay (μs)	275.1 ± 1.1	271.2 ± 0.82	225.5 ± 1.6
	Φ_0 (rad)	0	0	π
	Pole frequency (Hz)	–	–	3183.3 ± 98
	DAC anti-alias filter	See model in table 2		
	Pendulum	One 2nd order low-pass filter: $f_0=0.6$ Hz, $Q=1000$		
	χ^2/ndf	50.19/72	49.29.9/72	30.88.7/65

Table 3: ***WE (U-D coils), NE (U-D coils) and BS (four coils) mirror actuation parameterizations****, in LN1 mode. The parameterizations are valid up to 1 kHz and 2 kHz for the end mirrors and BS mirror respectively. The χ^2/ndf of the fits are given. The raw delay is the measured delay that includes the delay from the injection path to the DSP and the delay from the Pr_B1p channels sensing. The corrected delay takes as reference the correction channel in the DSP (i.e. Sc_WE_zCorr) and does not contain the B1 sensing delay nor the delay for the injection part (raw delay with 100 μs less for the PrCa to DSP delay and 49.3 μs less from the dark fringe sensing: delay = raw_delay − 100 − 49.3 μs). Applying these TFs to zCorr should enable to estimate the induced motion at absolute GPS time.*

		WE, L-R coils	NE, L-R coils
LN1	Gain (μm/V)	20.443 ± 0.024	22.707 ± 0.018
	Raw delay (μs)	(600.8 ± 1.1)	(596.1 ± 0.9)
	Delay (μs)	651.5 ± 1.1	646.8 ± 0.9
	Φ_0 (rad)	0	0
	Pole frequency (Hz)	39.354 ± 0.49	–
	Zero frequency (Hz)	40.123 ± 0.50	–
	Pendulum	One 2nd order low-pass filter: $f_0 = 0.6\,\mathrm{Hz}$, $Q = 1000$	
	χ^2/ndf	.3/88	77.17/72

Table 4: ***WE (L-R coils), NE (L-R coils) mirror actuation parameterizations****, in LN1 mode. The parameterizations are valid up to 1 kHz. The* χ^2/ndf *of the fits are given. The raw delay is the measured delay that includes the delay from the injection path (from PrCa) to the DSP and the delay from the* Pr_B1p *channels sensing. The corrected delay takes as reference the channels sent by the CaInjectors (i.e.* Ca_WE_zMirLR*) and does not contain the B1 sensing delay (raw delay with 100* μs *more since the hardware injections are done from the CaInjectors and* 49.3 μs *less from the dark fringe sensing: delay =* $raw\_delay + 100 - 49.3$ μs*). Applying these TFs to* Ca_WE_zMirLR *channels should enable to estimate the induced motion at absolute GPS time.*

	PR, four coils
Gain (μm/V)	14.26 ± 0.16
Raw delay (μs)	(612.2 ± 16)
Delay (μs)	462.9 ± 16
Φ_0 (rad)	π
Pole frequency (Hz)	77.7 ± 17
Zero frequency (Hz)	91.9 ± 22
Pendulum	One 2nd order low-pass filter: $f_0 = 0.6\,\mathrm{Hz}$, $Q = 1000$
χ^2/ndf	16.69/72

Table 5: ***PR (four coils) mirror actuation parameterization*** *in its single mode, valid up to 500 Hz. The* χ^2/ndf *of the fit is given. The raw delay is the measured delay that includes the delay from the injection path (from PrCa) to the DSP and the delay from the* Pr_B1p *channels sensing. The corrected delay takes as reference the correction channel in the DSP (i.e.* Sc_WE_zCorr*) and does not contain the B1 sensing delay nor the delay for the injection part (raw delay with 100* μs *less for the PrCa to DSP delay and* 49.3 μs *less from the dark fringe sensing:* $delay = raw\_delay - 100 - 49.3$ μs*). Applying these TFs to zCorr should enable to estimate the induced mirror motion at absolute GPS time.*

3.5 Figures

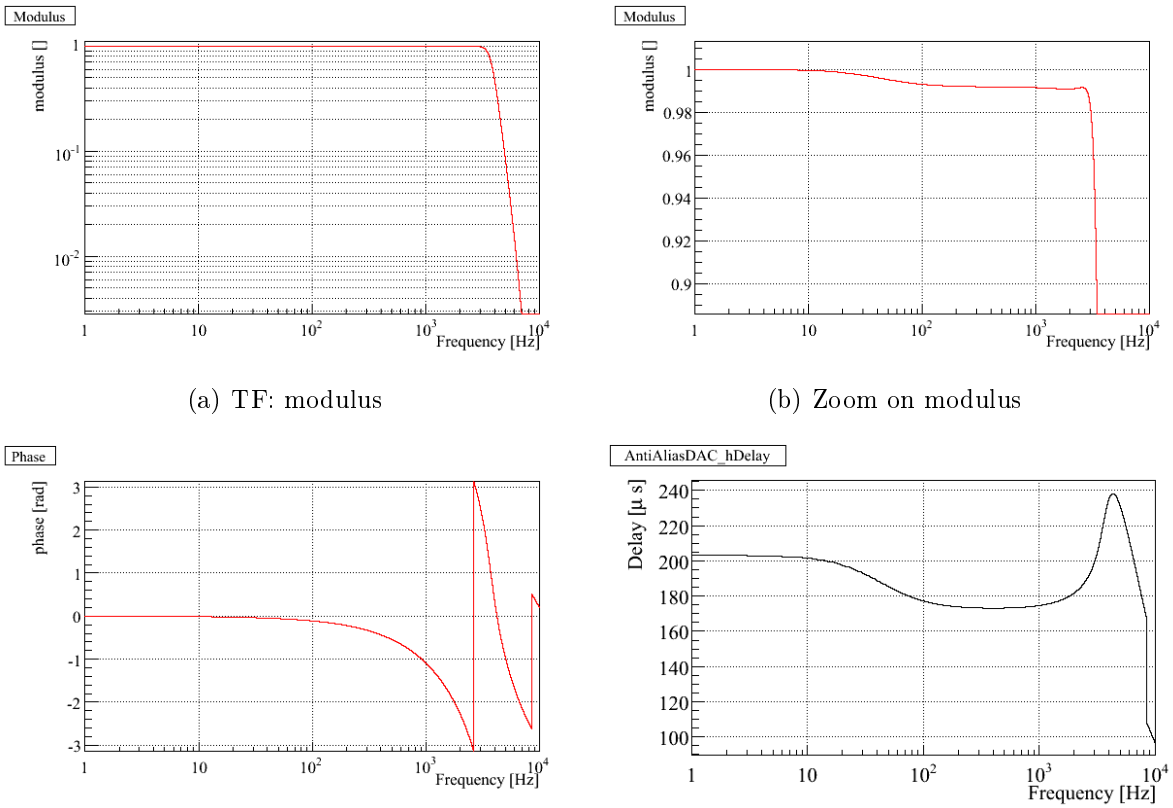

(a) TF: modulus

(b) Zoom on modulus

(c) TF: phase

(d) Equivalent delay

Figure 3: ***Model of the anti-imaging filter of the DAC.***

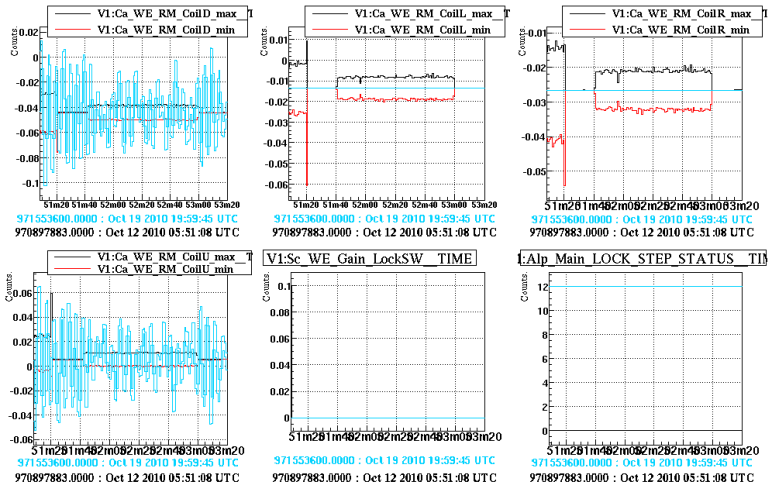

Figure 4: ***Levels of the load applied on the coils of WE mirror in LN1 mode****, during LN1 to HP measurements (black and red curves), and during Science Mode data (blue curves).*

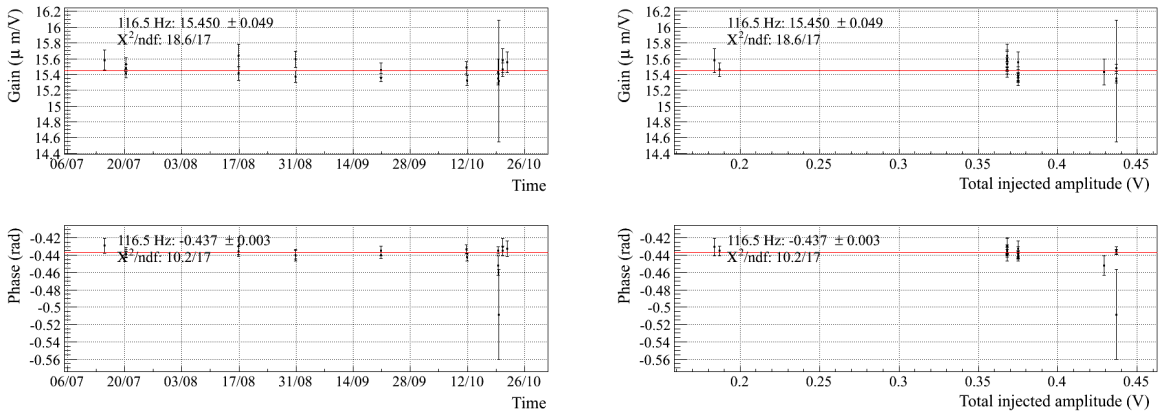

(a) vs time (b) vs excitation level

Figure 5: ***Stability and linearity of the mirror actuation in HP mode*** *(free swinging Michelson data). Example of the WE mirror actuation (U-D coils) at 116.5 Hz.*

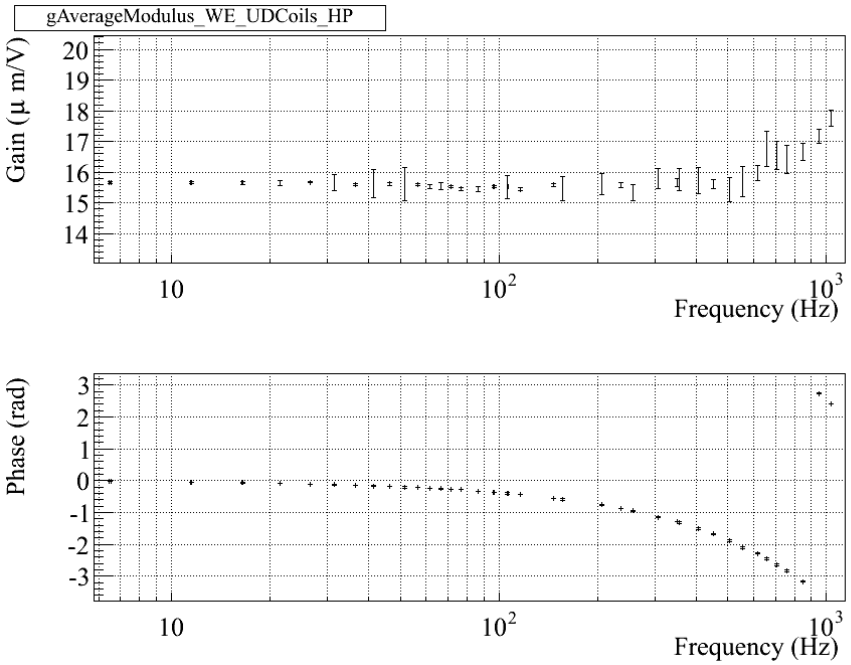

Figure 6: ***Measured actuation of the WE mirror using the U-D coils in HP mode.***

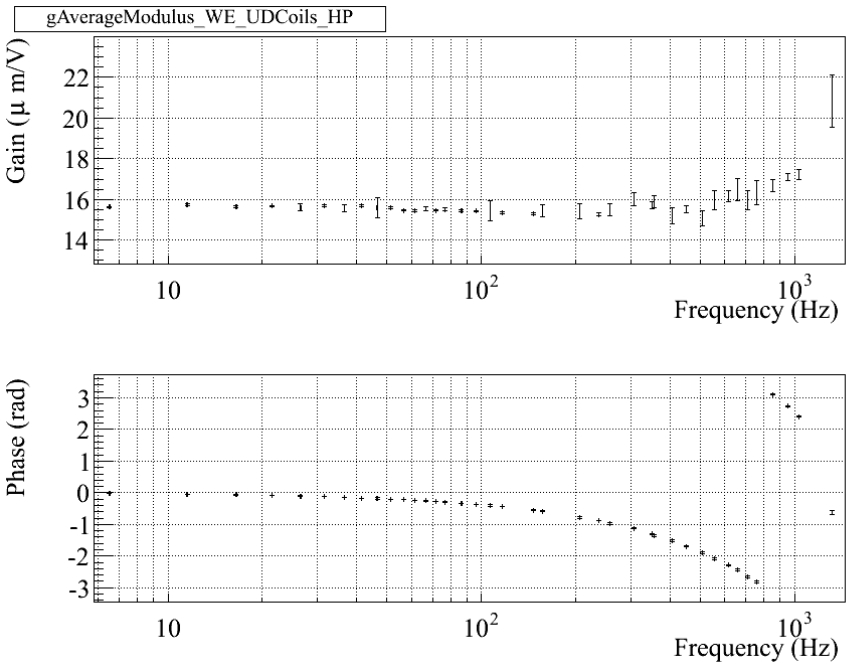

Figure 7: ***Measured actuation of the WE mirror using the L-R coils in HP mode.***

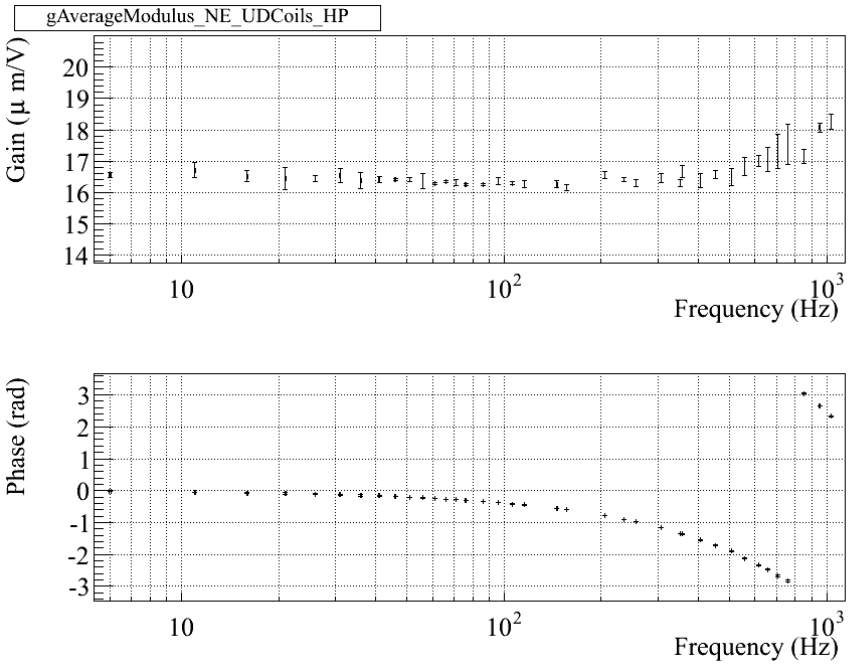

Figure 8: ***Measured actuation of the NE mirror using the U-D coils in HP mode.***

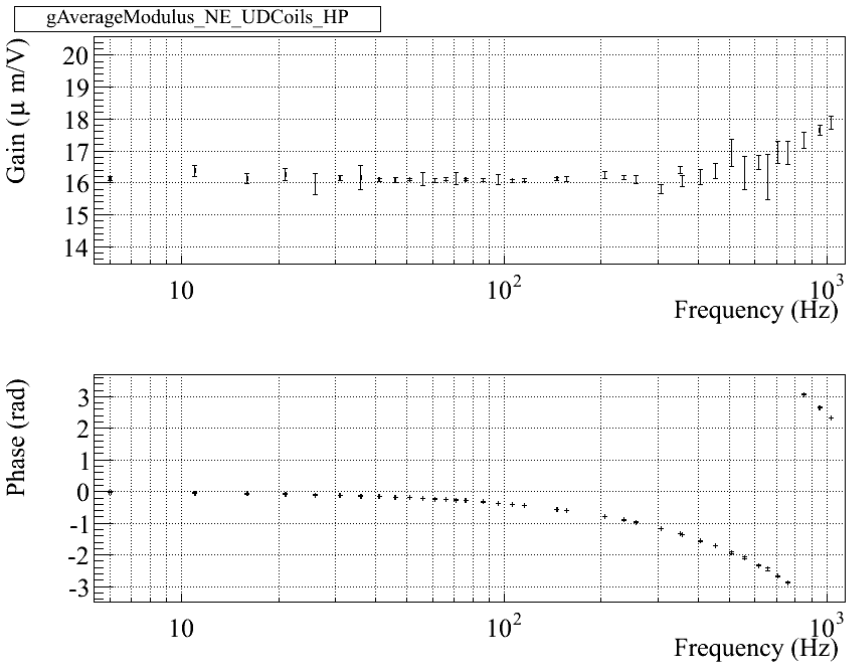

Figure 9: ***Measured actuation of the NE mirror using the L-R coils in HP mode.***

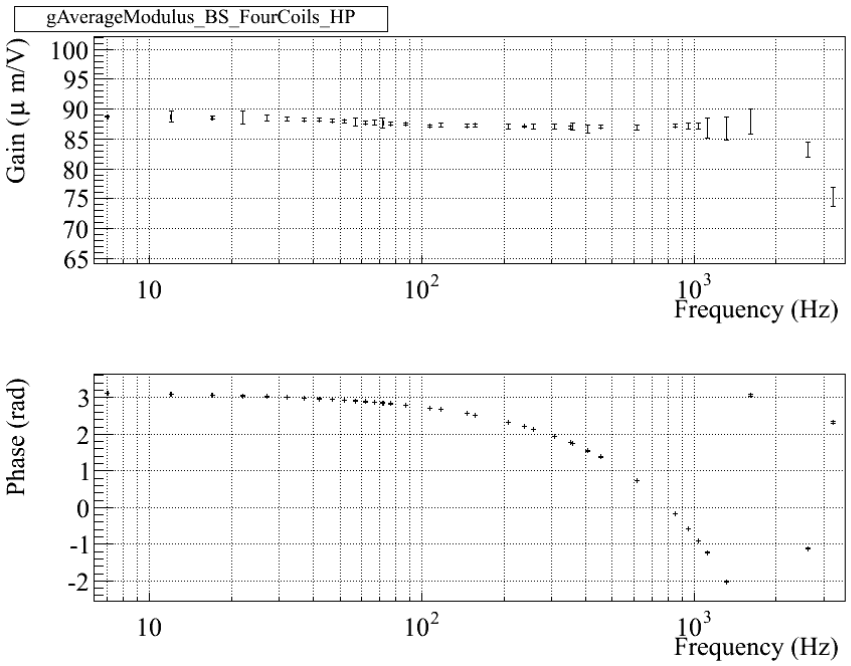

Figure 10: ***Measured actuation of the BS mirror using the four coils in HP mode.***

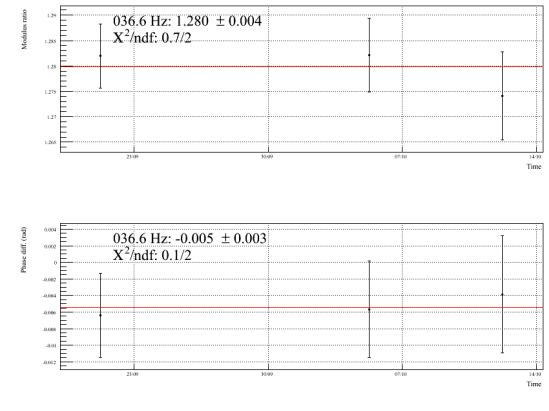

(a) 36.5 Hz

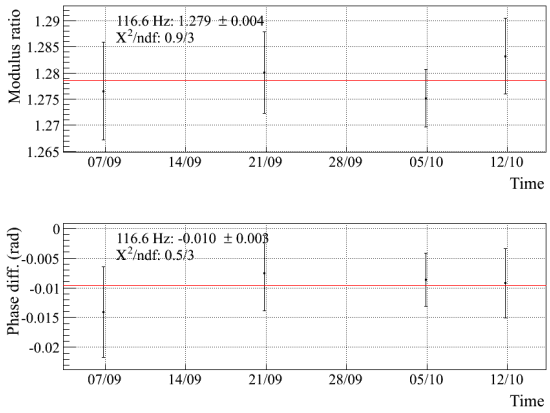

(b) 116.5 Hz

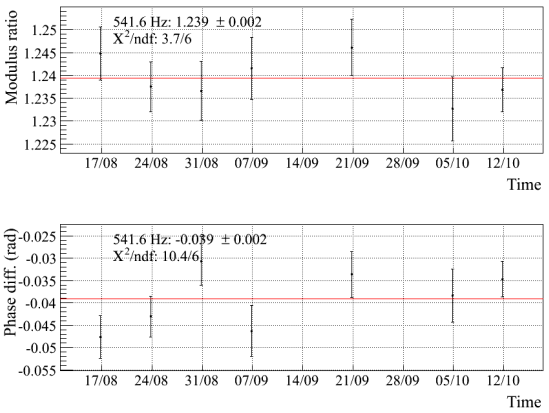

(c) 451.5 Hz

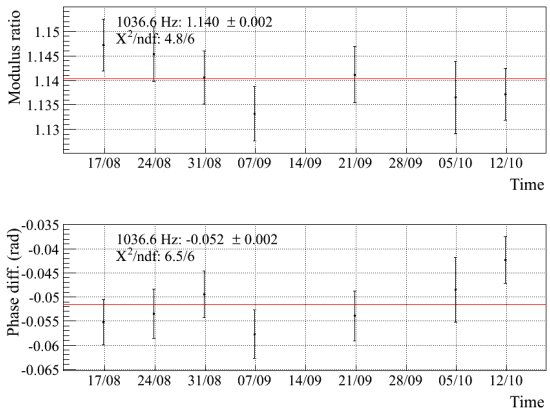

(d) 1036.5 Hz

Figure 11: ***Evolution as function of time of the measured actuation TF ratio (LN1/HP) for the up coil of the WE mirror*** *at four different frequencies.*

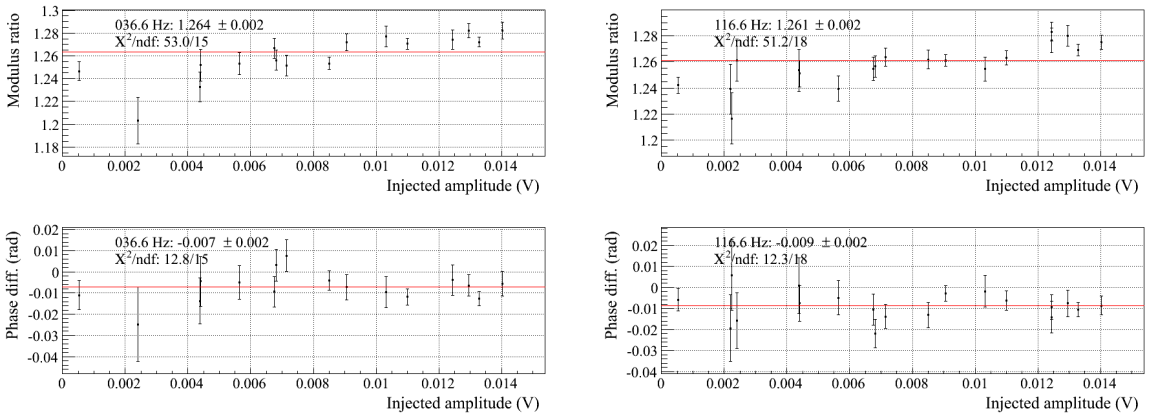

(a) 36.5 Hz

(b) 116.5 Hz

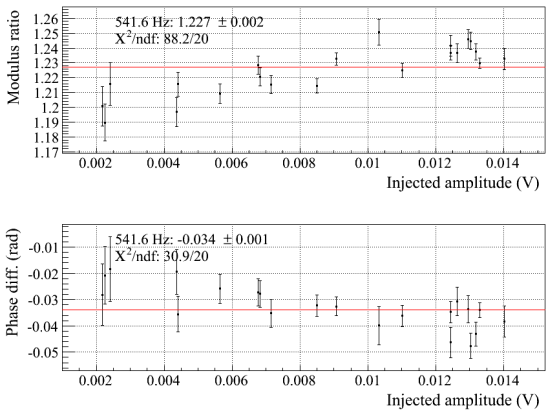

(c) 451.5 Hz

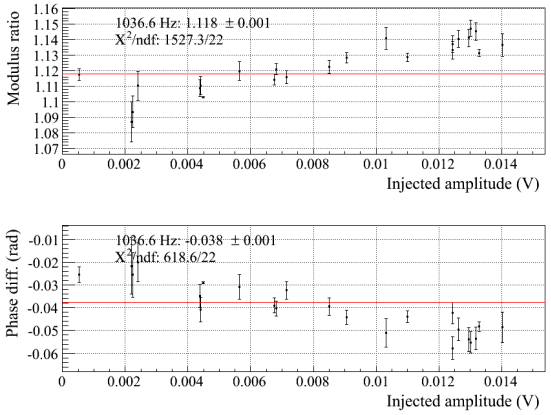

(d) 1036.5 Hz

Figure 12: ***Evolution as function of the signal amplitude of the measured actuation TF ratio (LN1/HP) for the up coil of the WE mirror*** *at four different frequencies. The amplitude in the x-axis is the amplitude of* $V1 : Ca\_WE\_RM\_CoilU$ *during the injections in LN1 mode.*

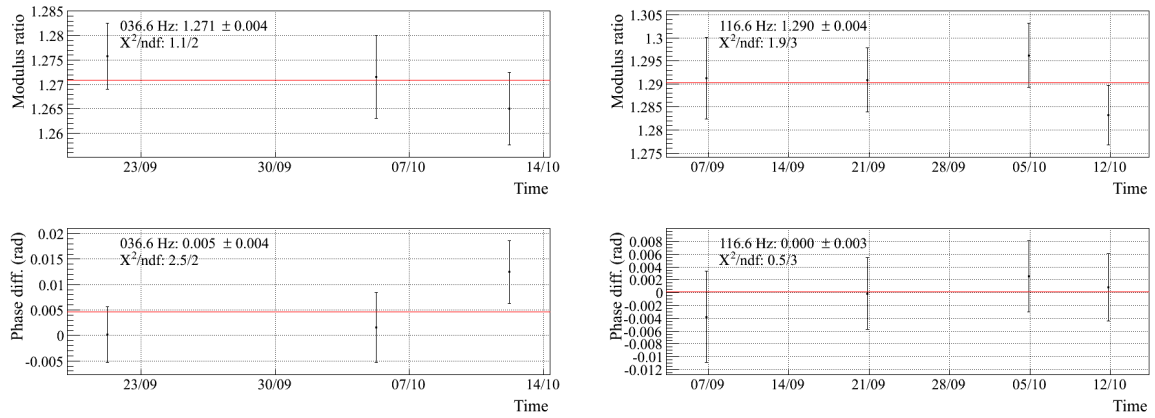

(a) 36.5 Hz (b) 116.5 Hz

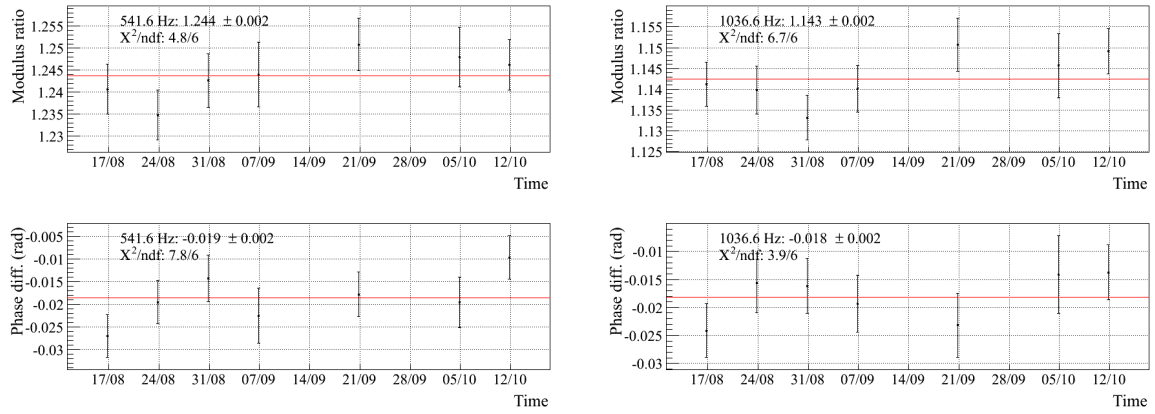

(c) 451.5 Hz (d) 1036.5 Hz

Figure 13: ***Evolution as function of time of the measured actuation TF ratio (LN1/HP) for the down coil of the WE mirror*** *at four different frequencies.*

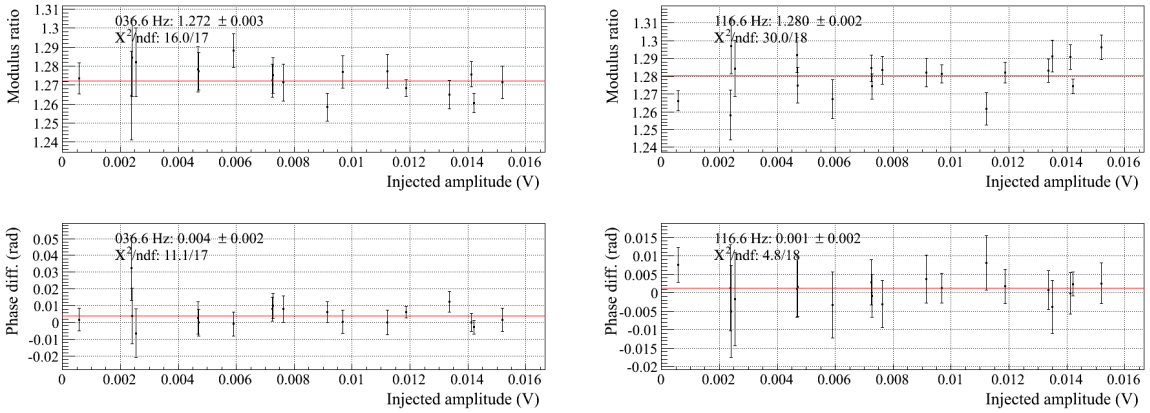

(a) 36.5 Hz

(b) 116.5 Hz

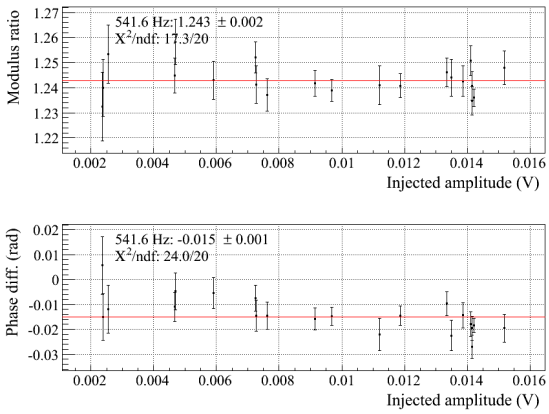

(c) 451.5 Hz

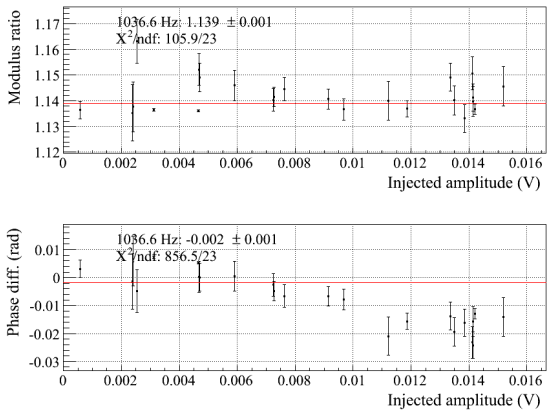

(d) 1036.5 Hz

Figure 14: ***Evolution as function of the signal amplitude of the measured actuation TF ratio (LN1/HP) for the down coil of the WE mirror*** *at four different frequencies. The amplitude in the x-axis is the amplitude of* $V1 : Ca\_WE\_RM\_CoilD$ *during the injections in LN1 mode.*

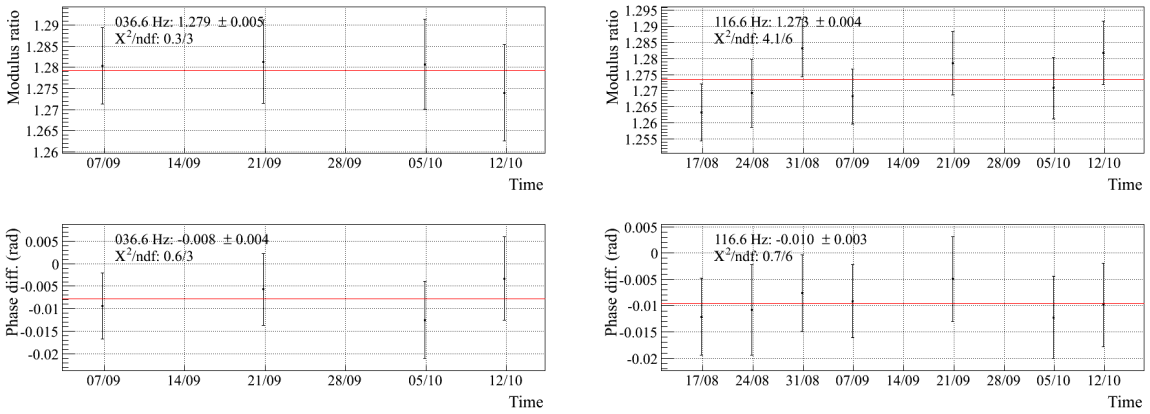

(a) 36.5 Hz

(b) 116.5 Hz

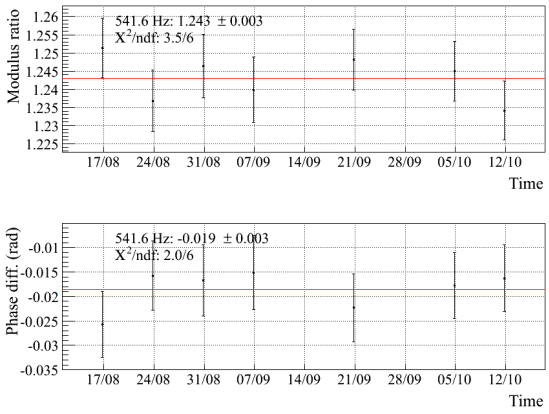

(c) 451.5 Hz

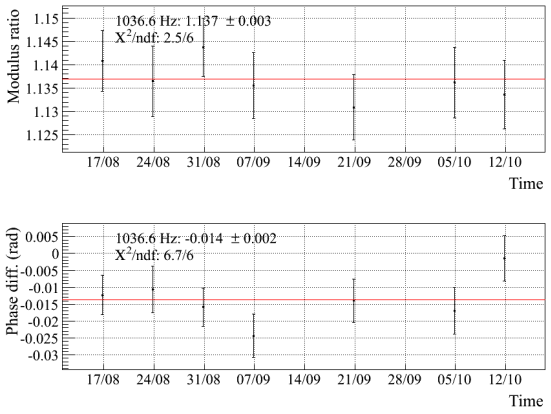

(d) 1036.5 Hz

Figure 15: ***Evolution as function of time of the measured actuation TF ratio (LN1/HP) for the left coil of the WE mirror*** *at four different frequencies.*

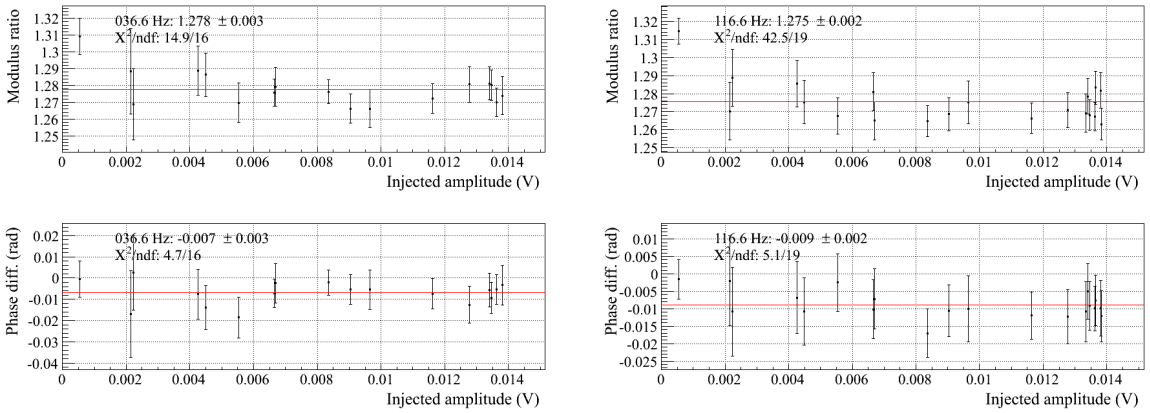

(a) 36.5 Hz

(b) 116.5 Hz

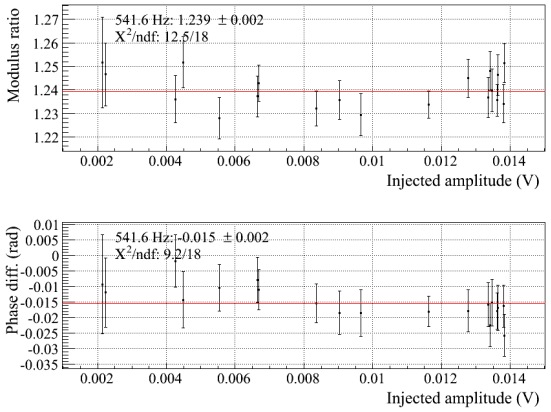

(c) 451.5 Hz

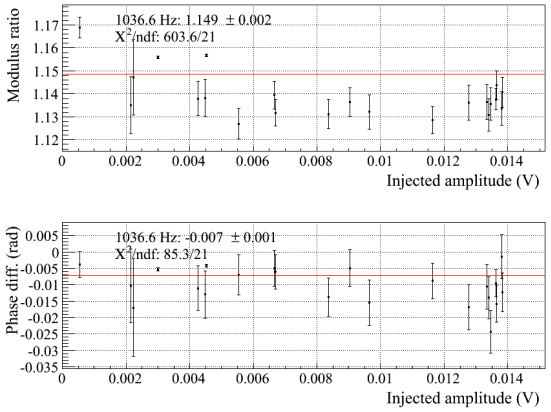

(d) 1036.5 Hz

Figure 16: ***Evolution as function of the signal amplitude of the measured actuation TF ratio (LN1/HP) for the laft coil of the WE mirror*** *at four different frequencies. The amplitude in the x-axis is the amplitude of* $V1 : Ca\_WE\_RM\_CoilL$ *during the injections in LN1 mode.*

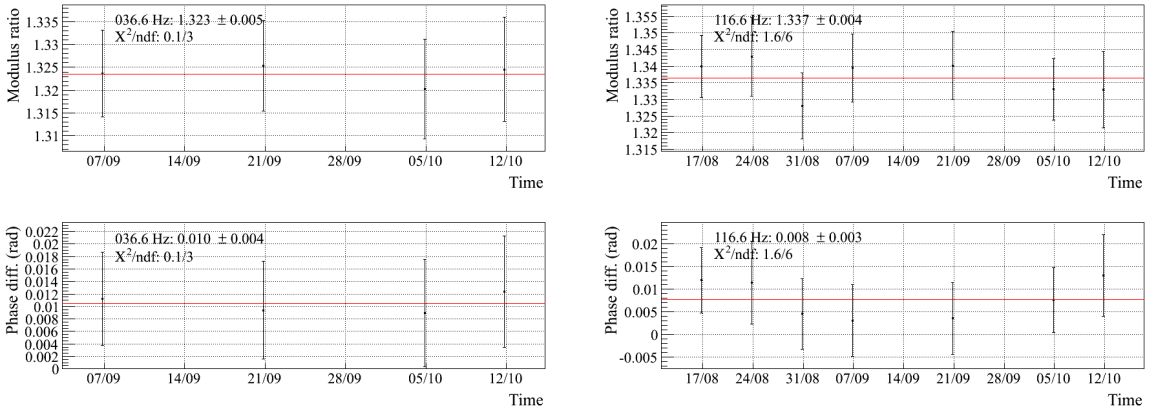

(a) 36.5 Hz

(b) 116.5 Hz

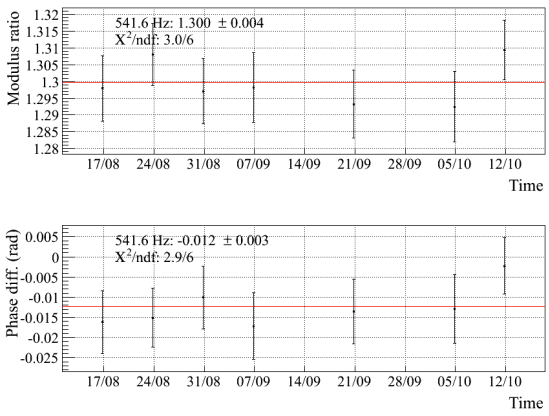

(c) 451.5 Hz

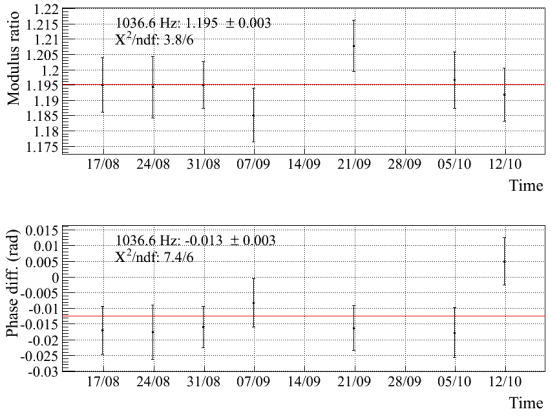

(d) 1036.5 Hz

Figure 17: ***Evolution as function of time of the measured actuation TF ratio (LN1/HP) for the right coil of the WE mirror*** *at four different frequencies.*

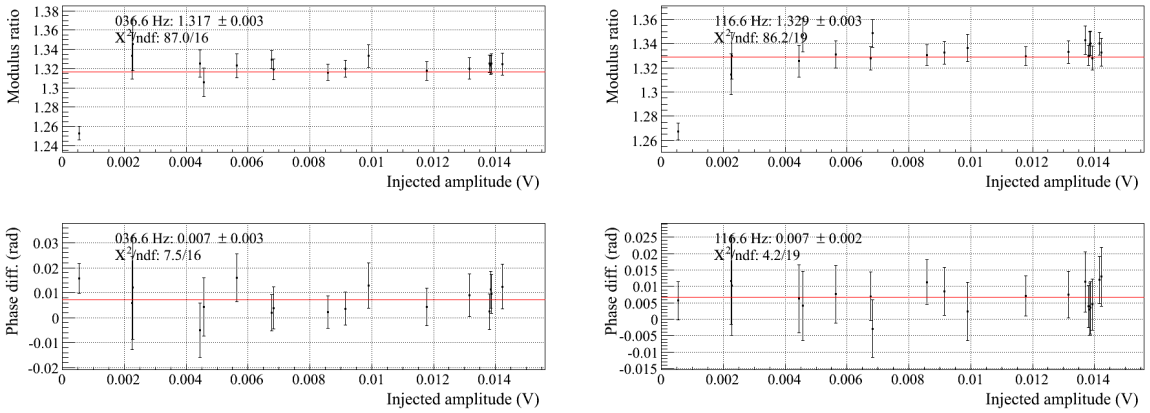

(a) 36.5 Hz

(b) 116.5 Hz

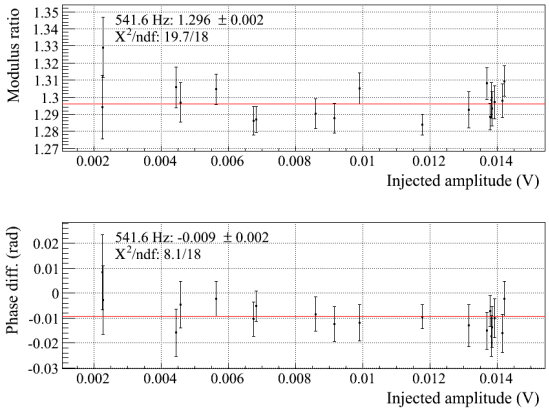

(c) 451.5 Hz

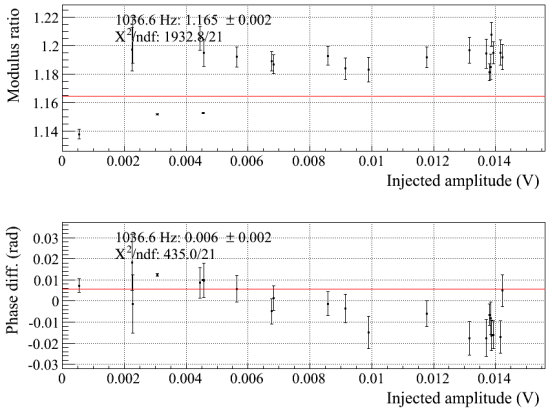

(d) 1036.5 Hz

Figure 18: ***Evolution as function of the signal amplitude of the measured actuation TF ratio (LN1/HP) for the right coil of the WE mirror*** *at four different frequencies. The amplitude in the x-axis is the amplitude of* $V1 : Ca\_WE\_RM\_CoilR$ *during the injections in LN1 mode.*

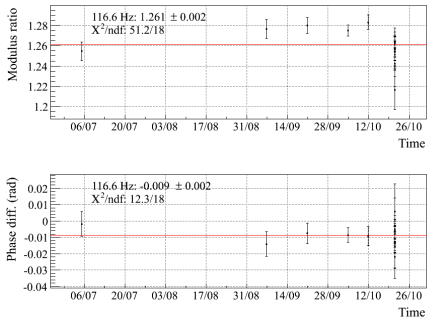

(a) Coil Up, 116.5 Hz.

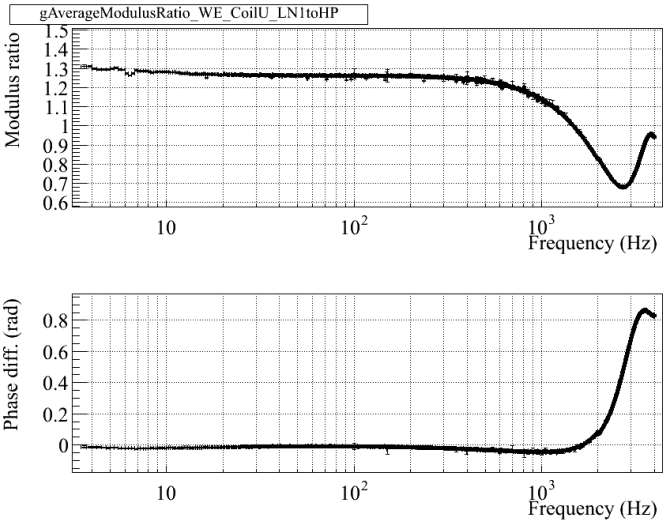

(b) Coil Up, averaged

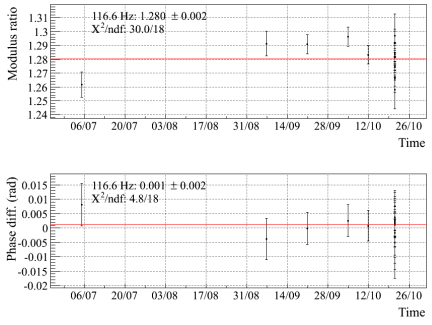

(c) Coil Down, 116.5 Hz

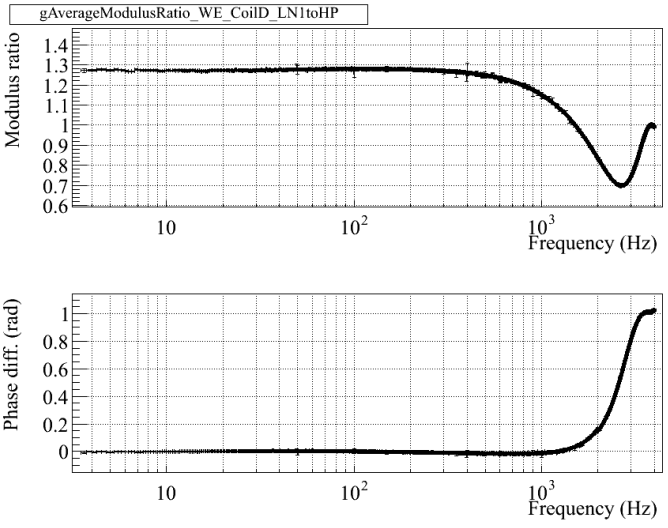

(d) Coil Down, averaged

Figure 19: ***Measured actuation TF ratio (LN1/HP) for the up and down coils of the WE mirror.***

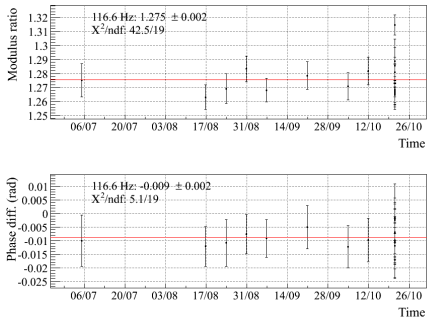

(a) Coil Left, 116.5 Hz

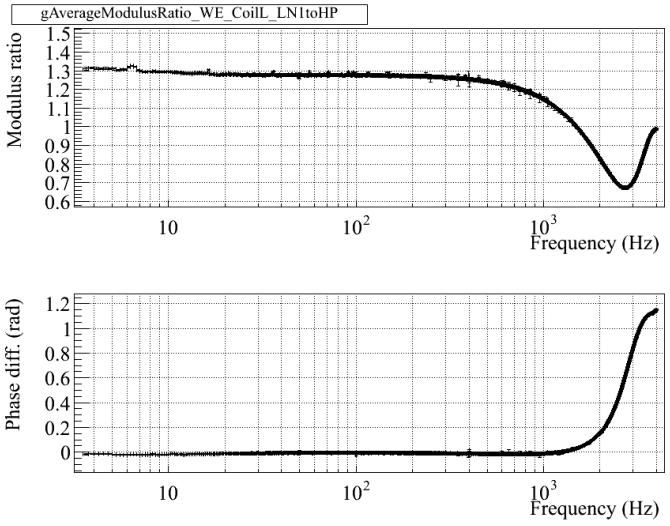

(b) Coil Left, averaged

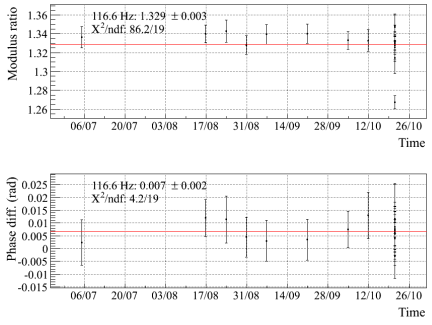

(c) Coil Right, 116.5 Hz

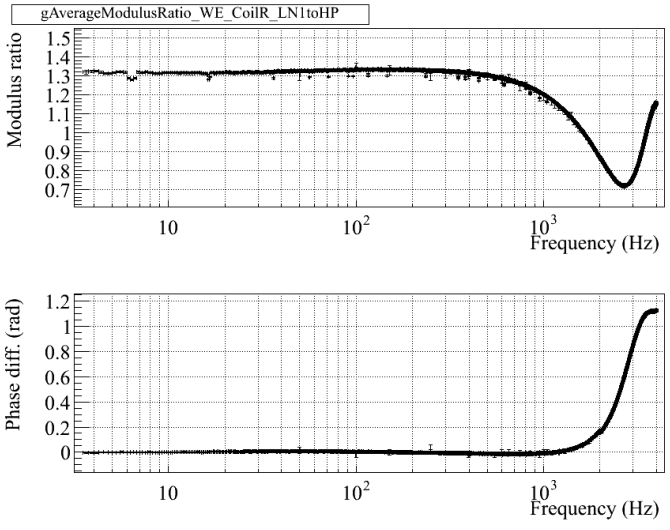

(d) Coil Right, averaged

Figure 20: ***Measured actuation TF ratio (LN1/HP) for the left and right coils of the WE mirror.***

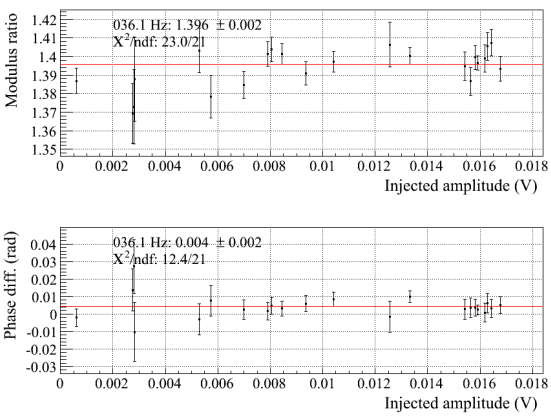

(a) 36.5 Hz

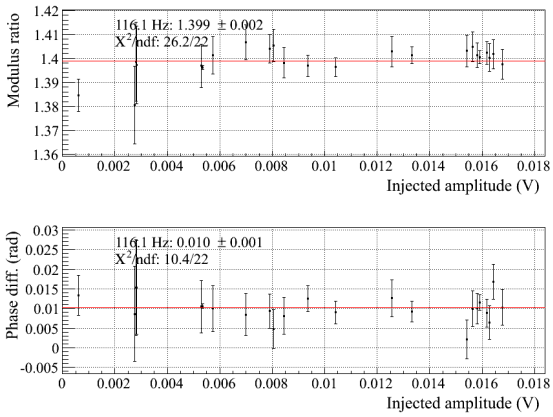

(b) 116.5 Hz

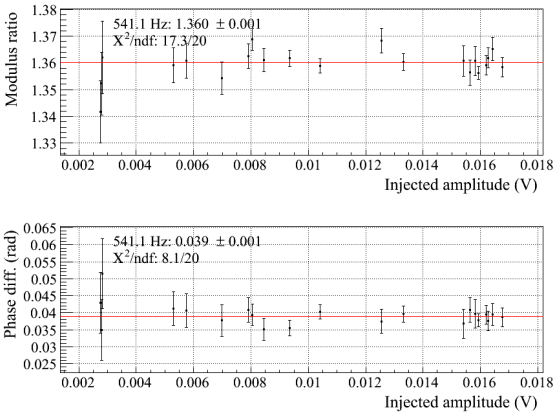

(c) 451.5 Hz

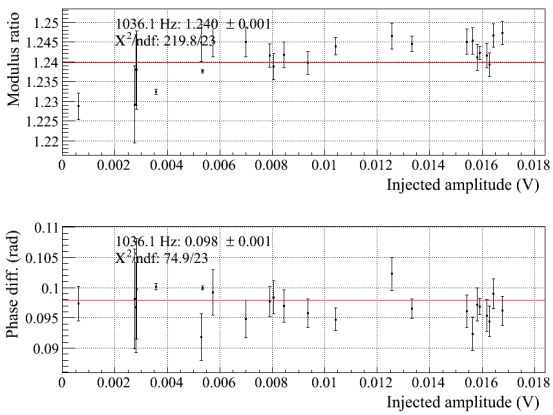

(d) 1036.5 Hz

Figure 21: ***Evolution as function of the signal amplitude of the measured actuation TF ratio (LN1/HP) for the up coil of the NE mirror*** *at four different frequencies. The amplitude in the x-axis is the amplitude of* $V1 : Ca\_NE\_RM\_CoilU$ *during the injections in LN1 mode.*

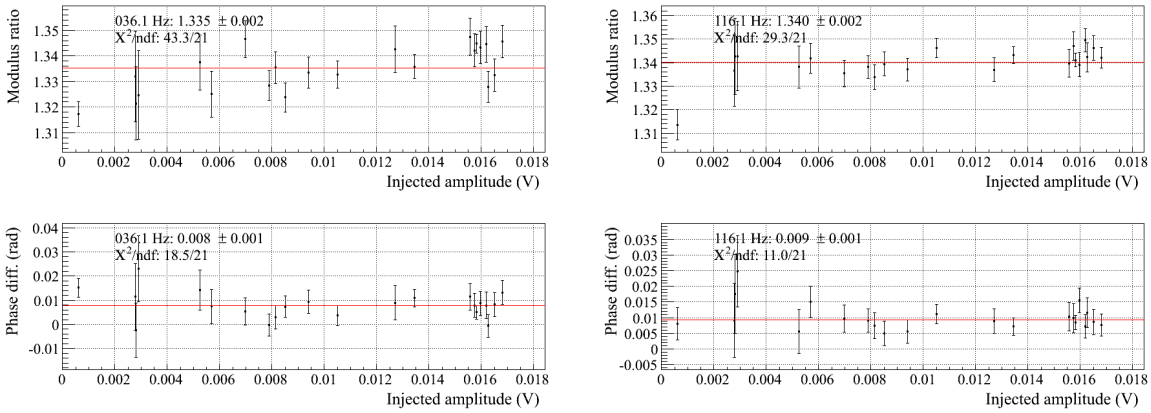

(a) 36.5 Hz

(b) 116.5 Hz

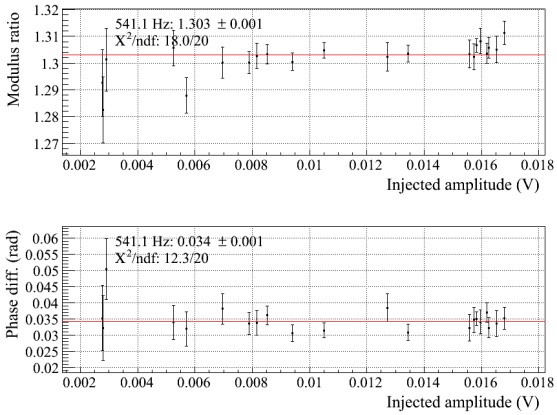

(c) 451.5 Hz

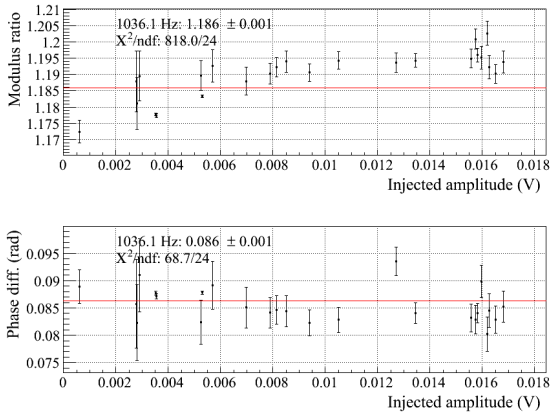

(d) 1036.5 Hz

Figure 22: ***Evolution as function of the signal amplitude of the measured actuation TF ratio (LN1/HP) for the down coil of the NE mirror*** *at four different frequencies. The amplitude in the x-axis is the amplitude of* $V1 : Ca\_NE\_RM\_CoilD$ *during the injections in LN1 mode.*

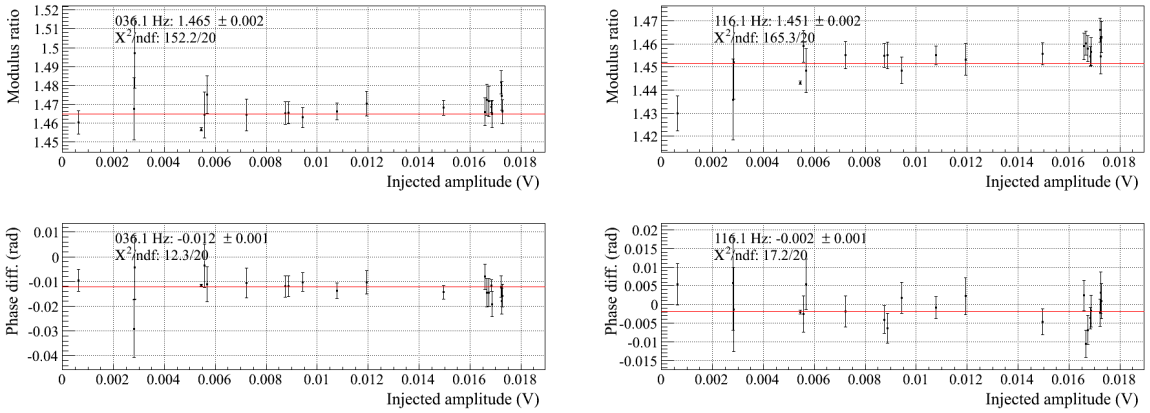

(a) 36.5 Hz

(b) 116.5 Hz

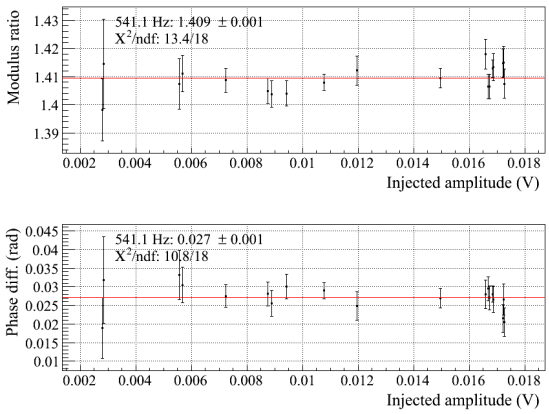

(c) 451.5 Hz

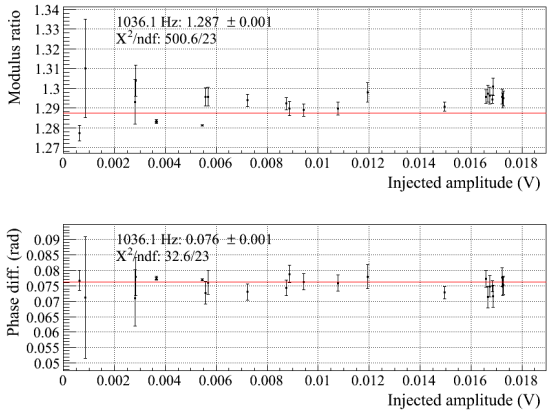

(d) 1036.5 Hz

Figure 23: ***Evolution as function of the signal amplitude of the measured actuation TF ratio (LN1/HP) for the left coil of the NE mirror*** *at four different frequencies. The amplitude in the x-axis is the amplitude of* $V1 : Ca\_NE\_RM\_CoilL$ *during the injections in LN1 mode.*

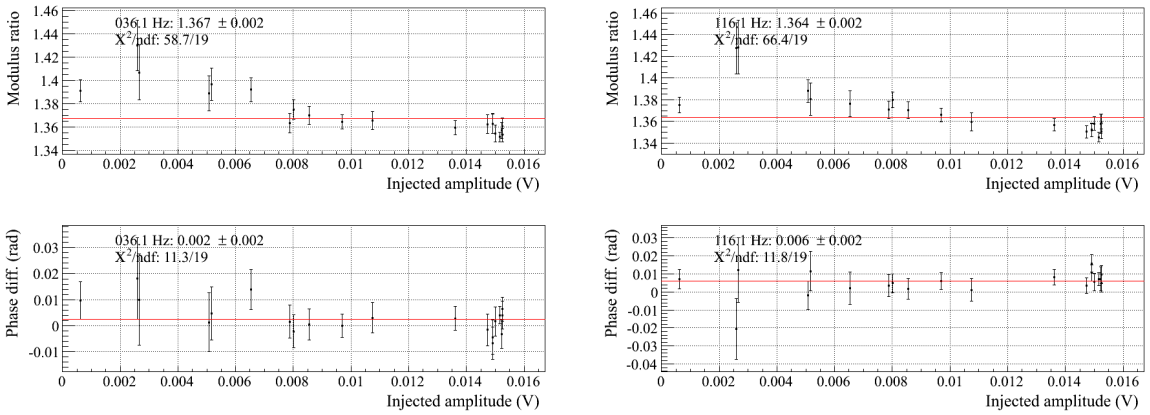

(a) 36.5 Hz

(b) 116.5 Hz

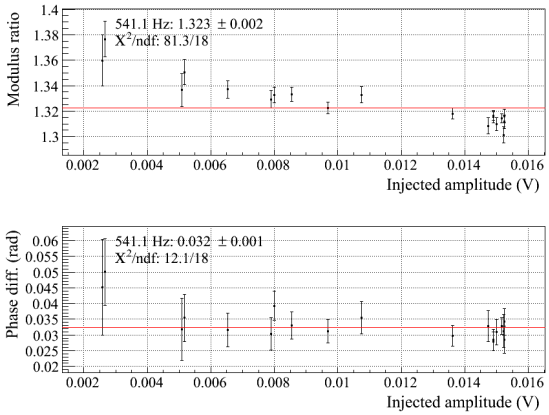

(c) 451.5 Hz

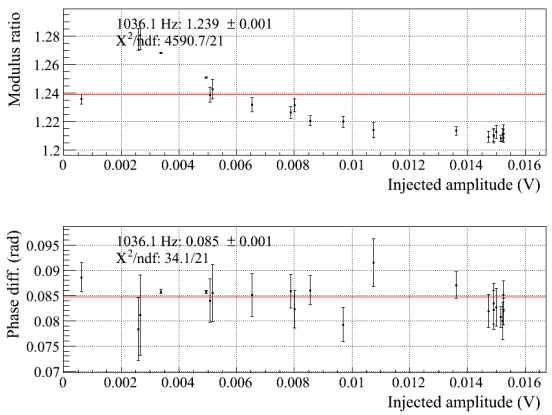

(d) 1036.5 Hz

Figure 24: ***Evolution as function of the signal amplitude of the measured actuation TF ratio (LN1/HP) for the right coil of the NE mirror*** *at four different frequencies. The amplitude in the x-axis is the amplitude of* $V1 : Ca\_NE\_RM\_CoilR$ *during the injections in LN1 mode.*

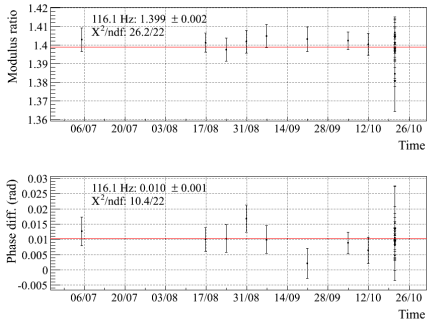

(a) Coil Up, 116.0 Hz

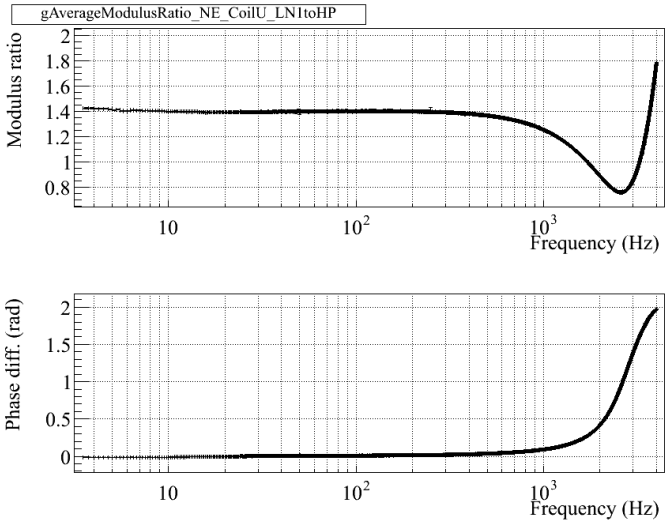

(b) Coil Up, averaged

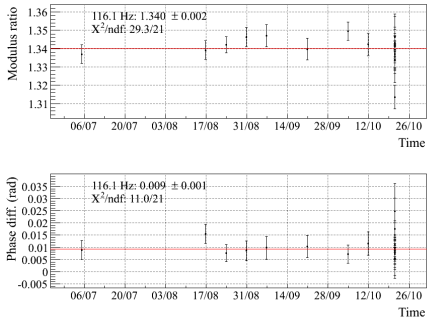

(c) Coil Down, 116.0 Hz

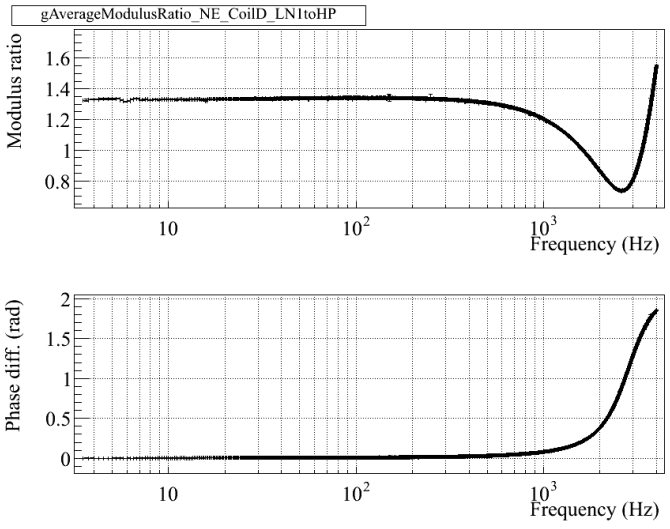

(d) Coil Down, averaged

Figure 25: ***Measured actuation TF ratio (LN1/HP) for the up and down coils of the NE mirror.***

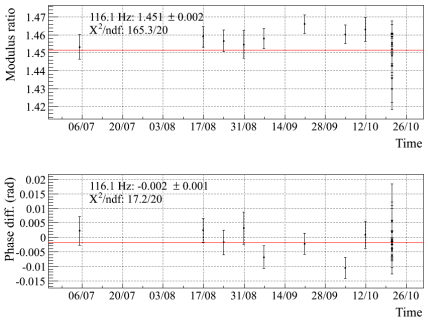

(a) Coil Left, 116.0 Hz

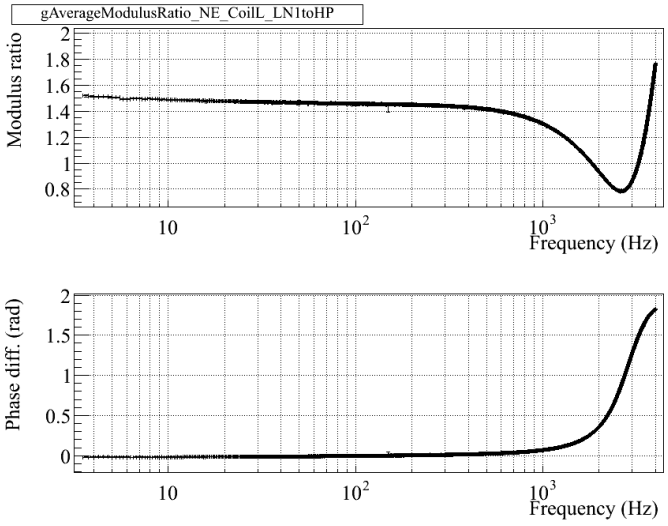

(b) Coil Left, averaged

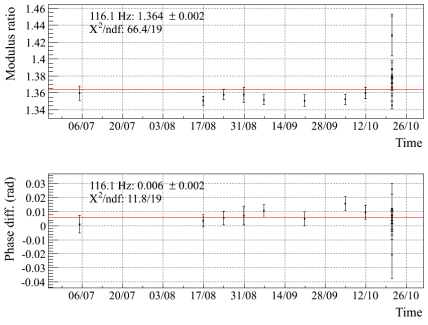

(c) Coil Right, 116.0

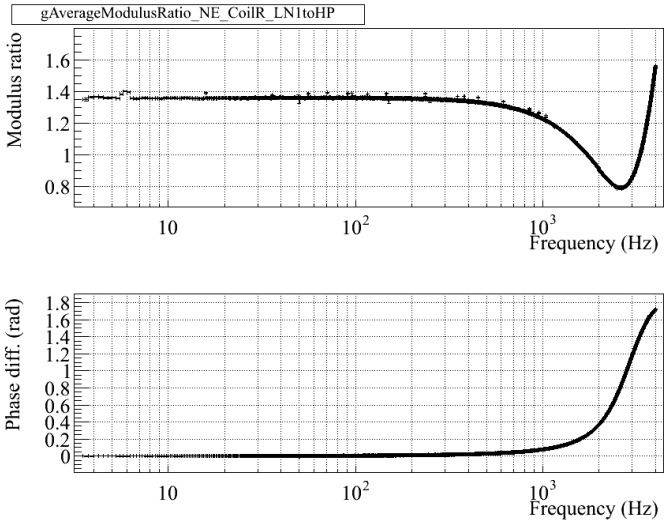

(d) Coil Right, averaged

Figure 26: ***Measured actuation TF ratio (LN1/HP) for the left and right coils of the NE mirror.***

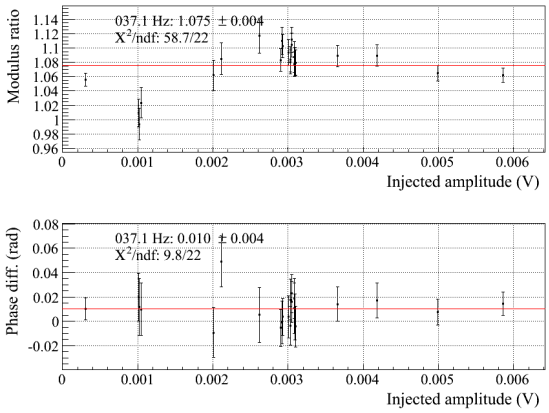

(a) 36.5 Hz

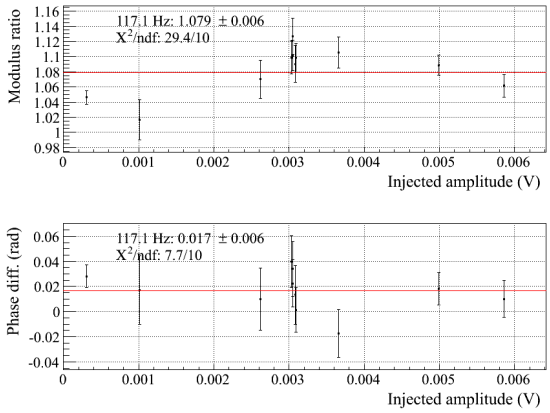

(b) 116.5 Hz

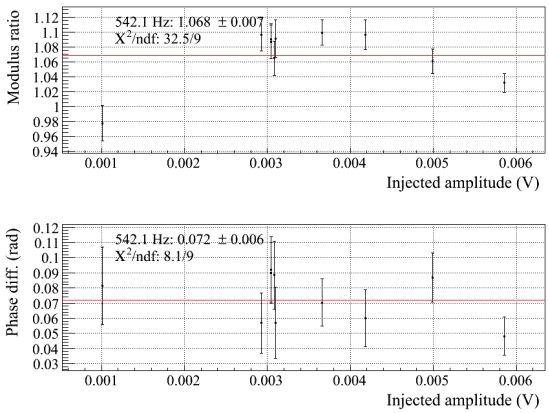

(c) 451.5 Hz

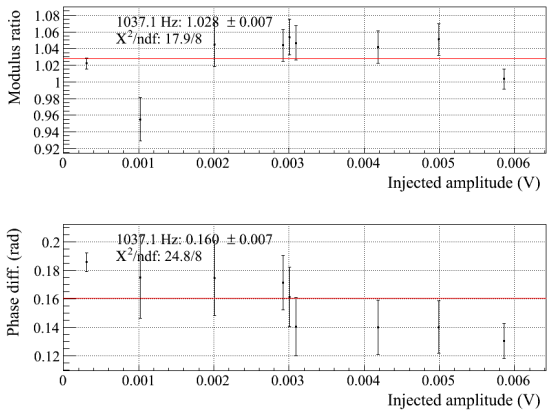

(d) 1036.5 Hz

Figure 27: ***Evolution as function of the signal amplitude of the measured actuation TF ratio (LN1/HP) for the up-left coil of the BS mirror*** *at four different frequencies. The amplitude in the x-axis is the amplitude of* $V1 : Ca\_BS\_RM\_CoilUL$ *during the injections in LN1 mode.*

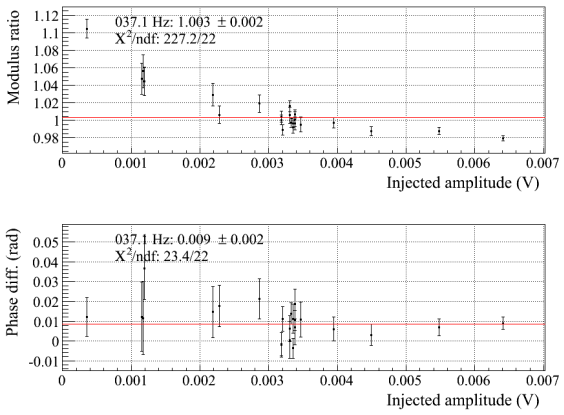

(a) 36.5 Hz

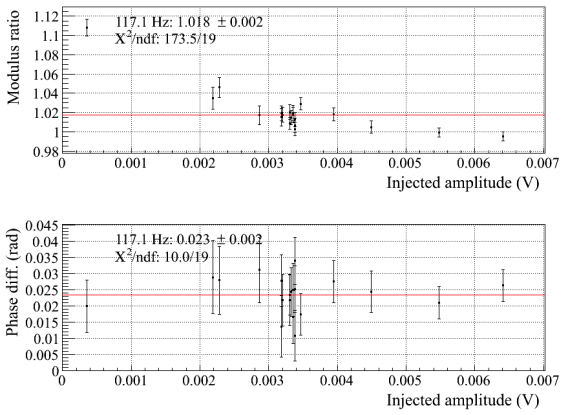

(b) 116.5 Hz

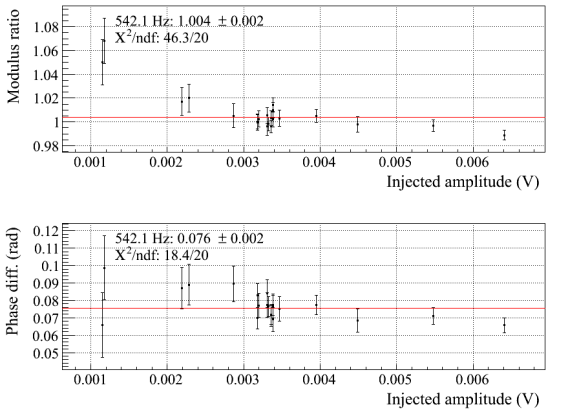

(c) 451.5 Hz

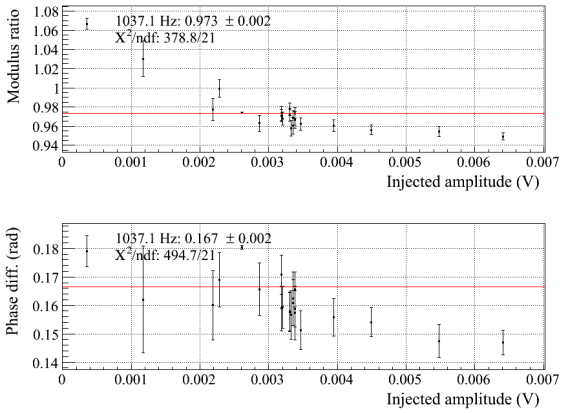

(d) 1036.5 Hz

Figure 28: ***Evolution as function of the signal amplitude of the measured actuation TF ratio (LN1/HP) for the down-left coil of the BS mirror*** *at four different frequencies. The amplitude in the x-axis is the amplitude of* $V1 : Ca\_BS\_RM\_CoilDL$ *during the injections in LN1 mode.*

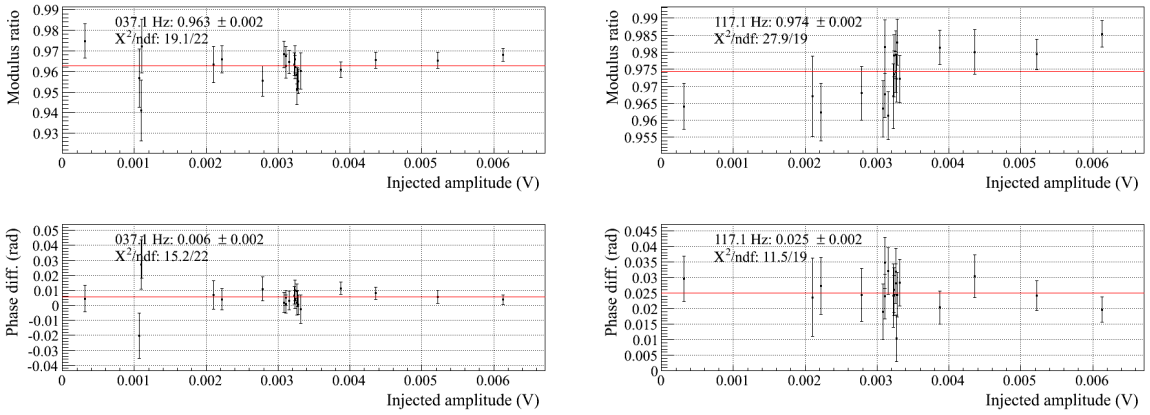

(a) 36.5 Hz

(b) 116.5 Hz

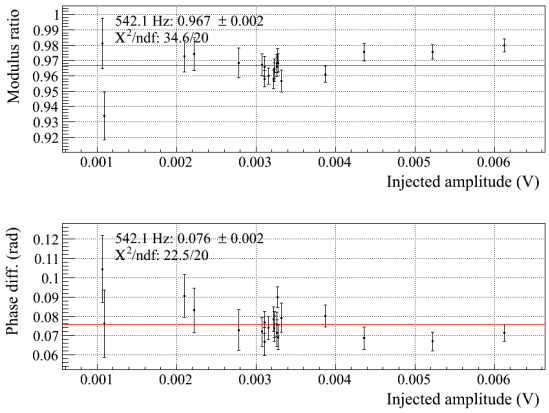

(c) 451.5 Hz

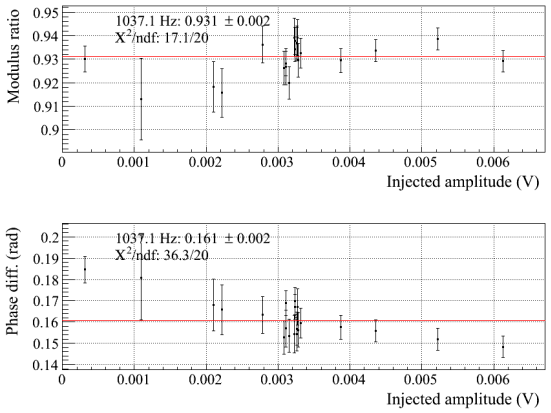

(d) 1036.5 Hz

Figure 29: ***Evolution as function of the signal amplitude of the measured actuation TF ratio (LN1/HP) for the up-right coil of the BS mirror*** *at four different frequencies. The amplitude in the x-axis is the amplitude of* $V1 : Ca\_BS\_RM\_CoilUR$ *during the injections in LN1 mode.*

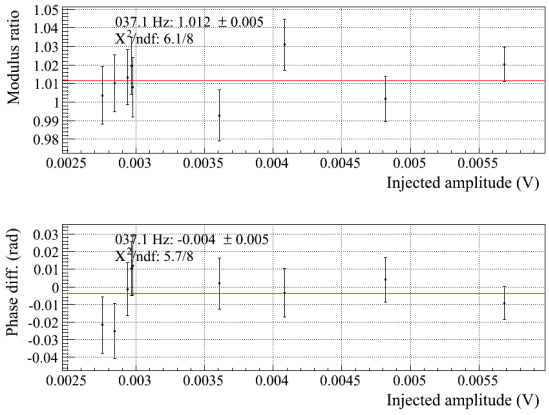

(a) 36.5 Hz

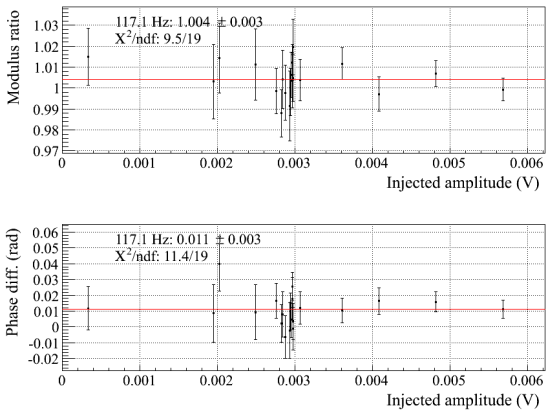

(b) 116.5 Hz

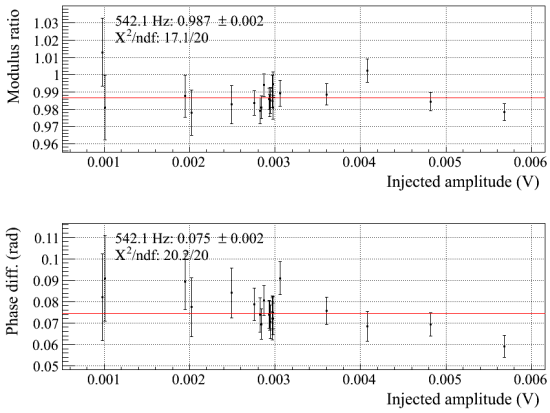

(c) 451.5 Hz

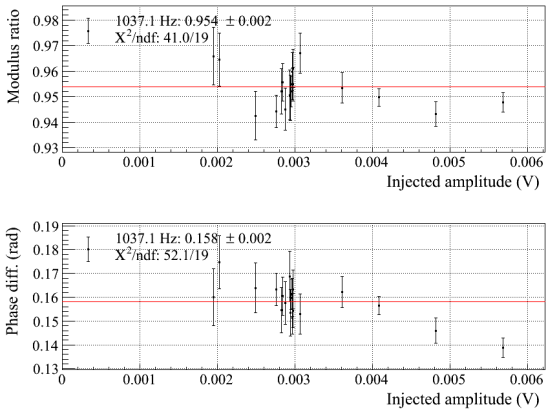

(d) 1036.5 Hz

Figure 30: ***Evolution as function of the signal amplitude of the measured actuation TF ratio (LN1/HP) for the down-ritht coil of the BS mirror*** *at four different frequencies. The amplitude in the x-axis is the amplitude of* $V1 : Ca\_BS\_RM\_CoilDR$ *during the injections in LN1 mode.*

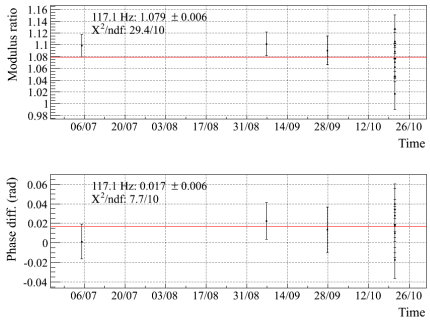

(a) Coil Up-Left, 117.0 Hz

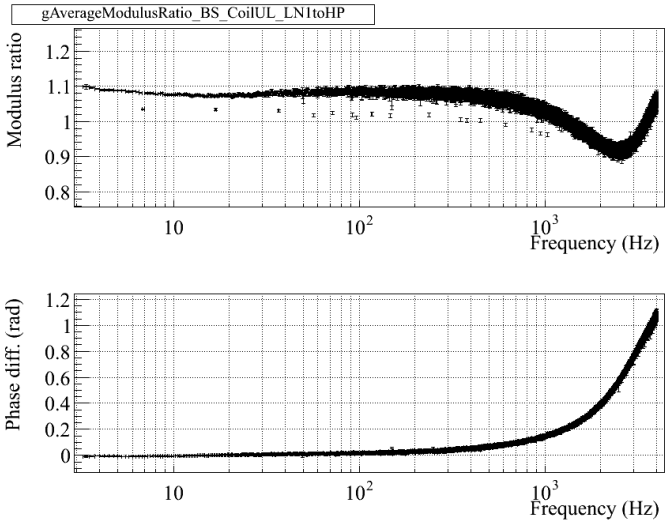

(b) Coil Up-Left, averaged

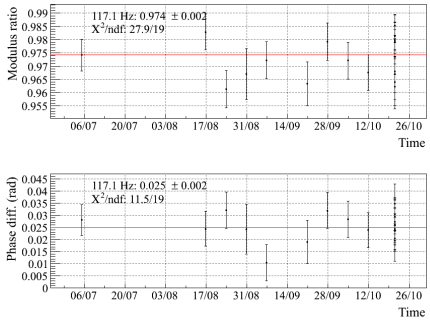

(c) Coil Up-Right, 117.0 Hz

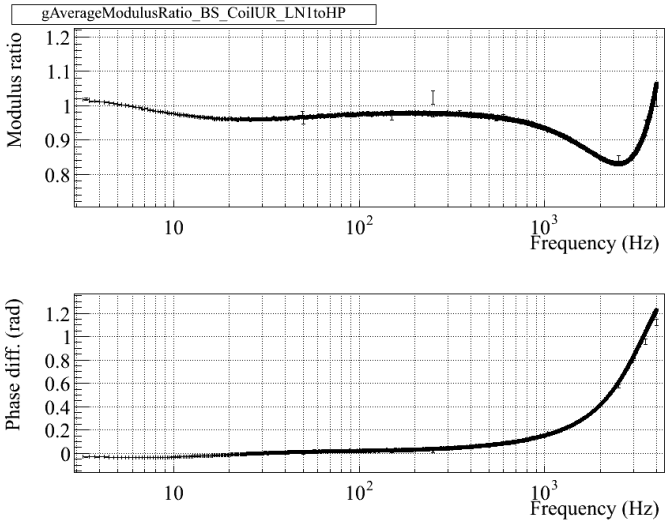

(d) Coil Up-Right, averaged

Figure 31: ***Measured actuation TF ratio (LN1/HP) for the up-left and up-right coils of the BS mirror.***

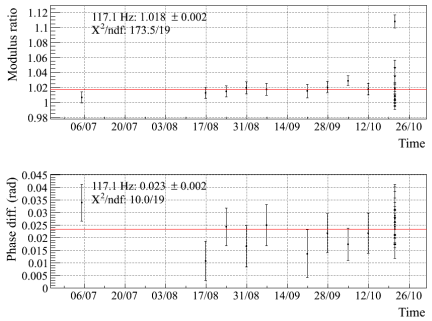

(a) Coil Down-Left, 117.0 Hz

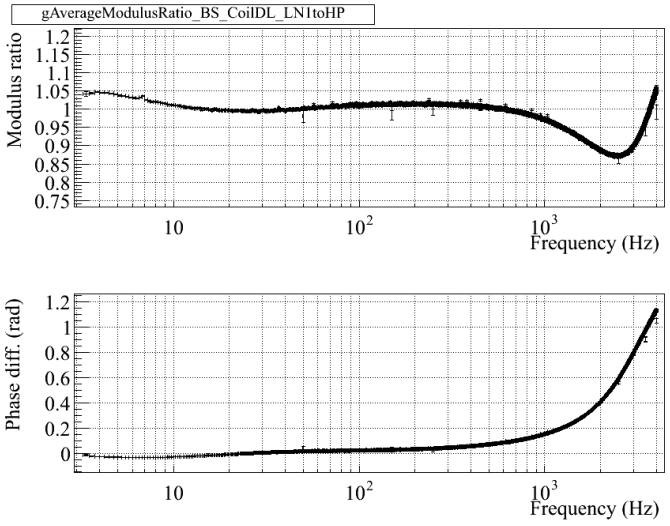

(b) Coil Down-Left, averaged

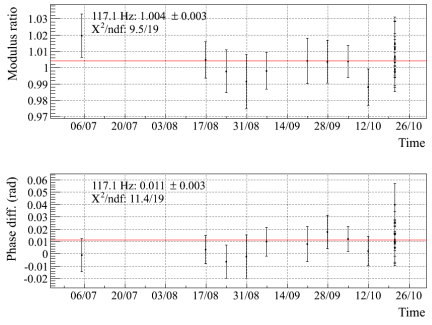

(c) Coil Down-Right, 117.0 Hz

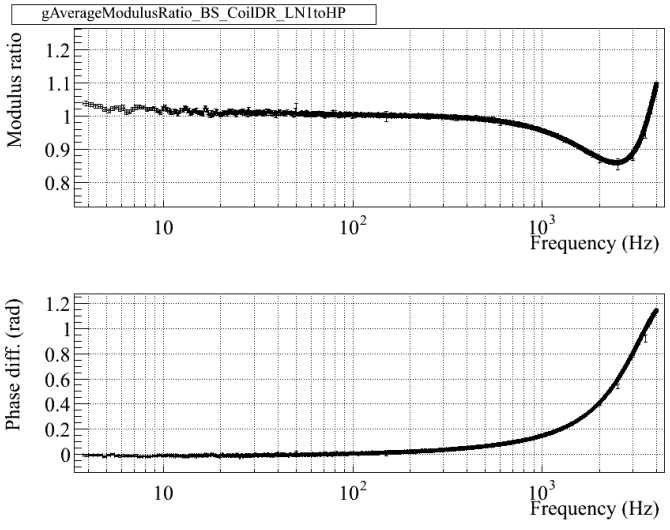

(d) Coil Down-Right, averaged

Figure 32: ***Measured actuation TF ratio (LN1/HP) for the down-left and down-right coils of the BS mirror.***

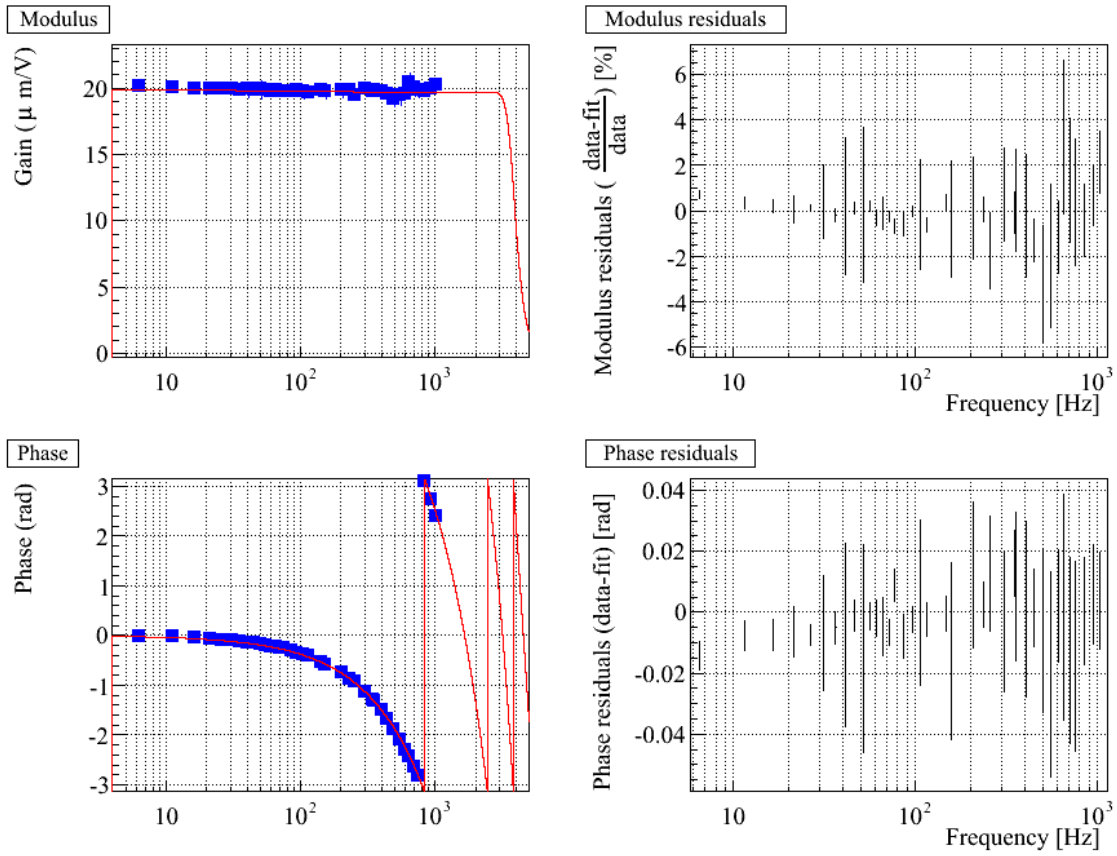

Figure 33: 1

Measured actuation of the WE mirror using the U-D coils in LN1 mode, fitted model and residuals.

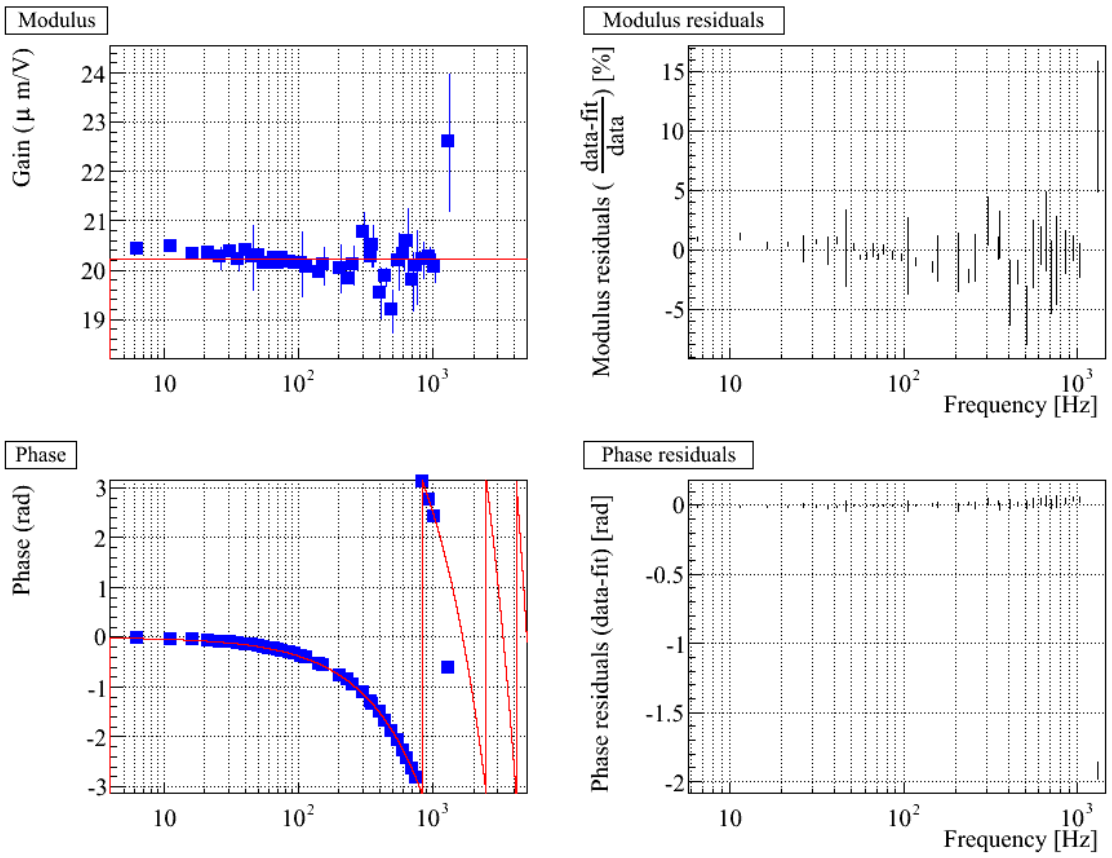

Figure 34: ***Measured actuation of the WE mirror using the L-R coils in LN1 mode****, fitted model and residuals.*

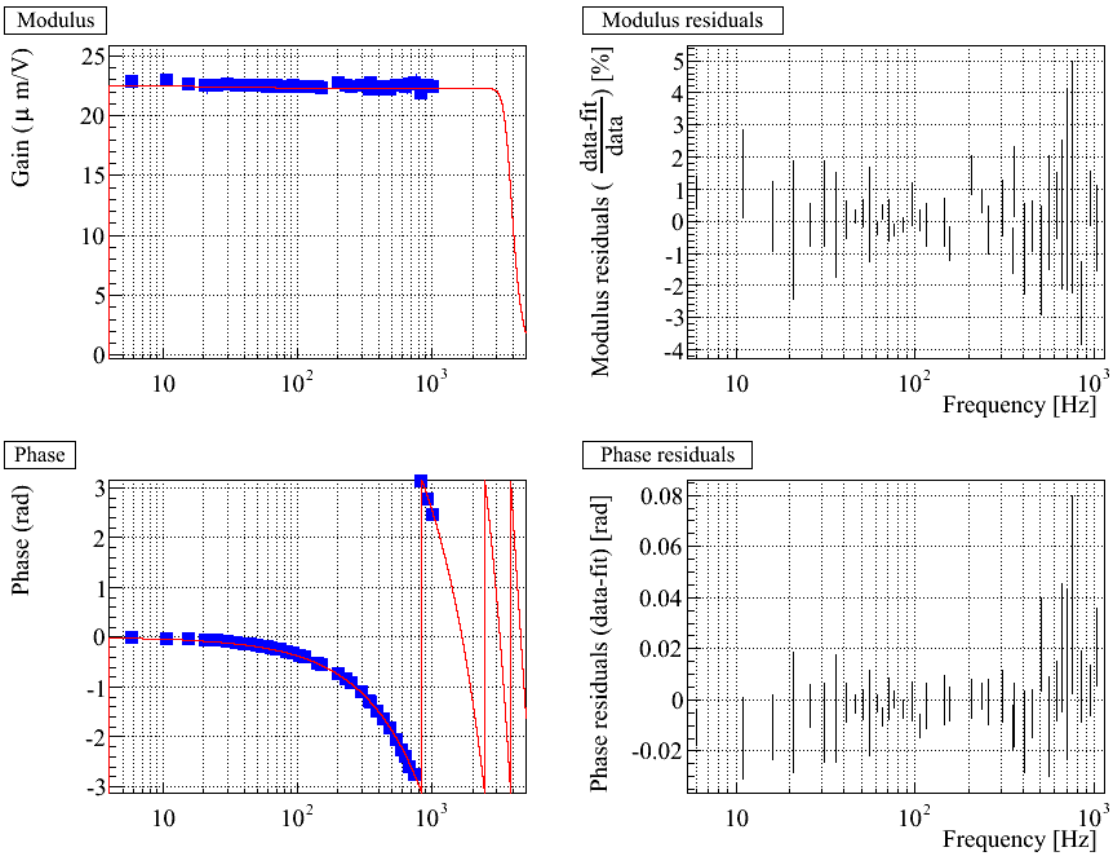

Figure 35: ***Measured actuation of the NE mirror using the U-D coils in LN1 mode****, fitted model and residuals.*

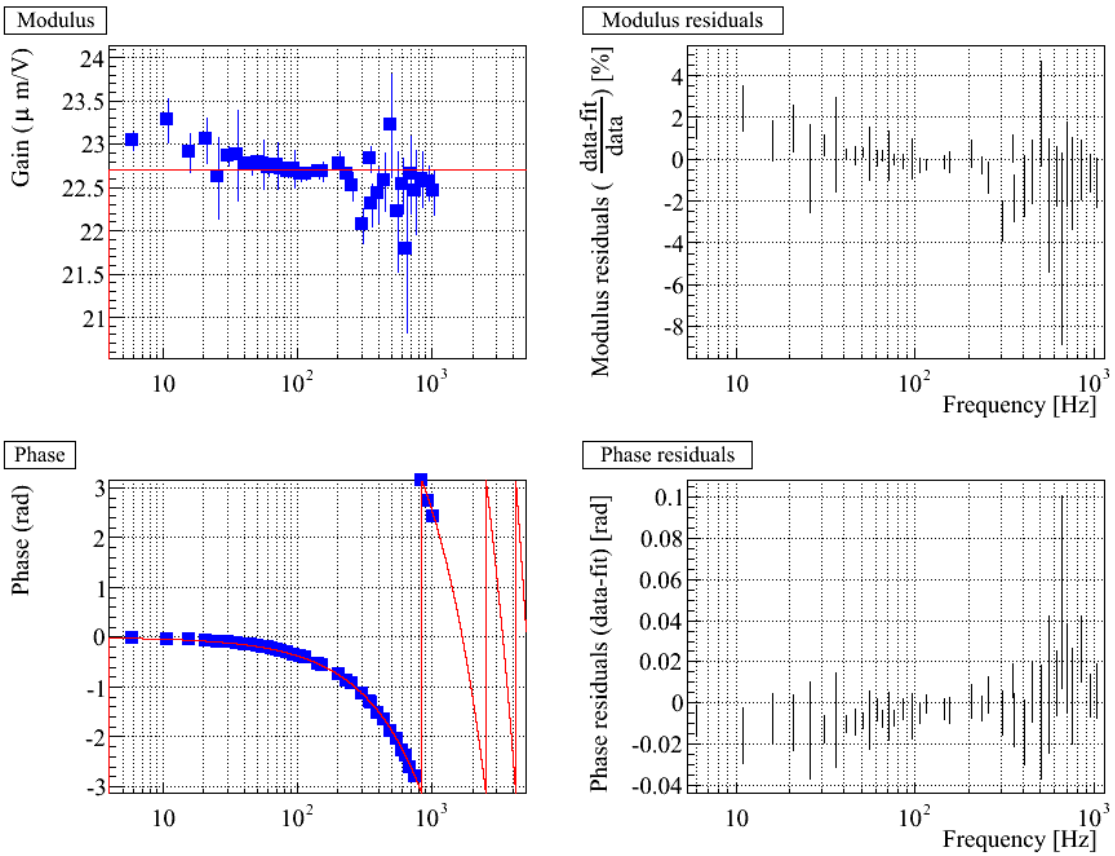

Figure 36: ***Measured actuation of the NE mirror using the L-R coils in LN1 mode****, fitted model and residuals. The data have been fitted below 400 Hz only.*

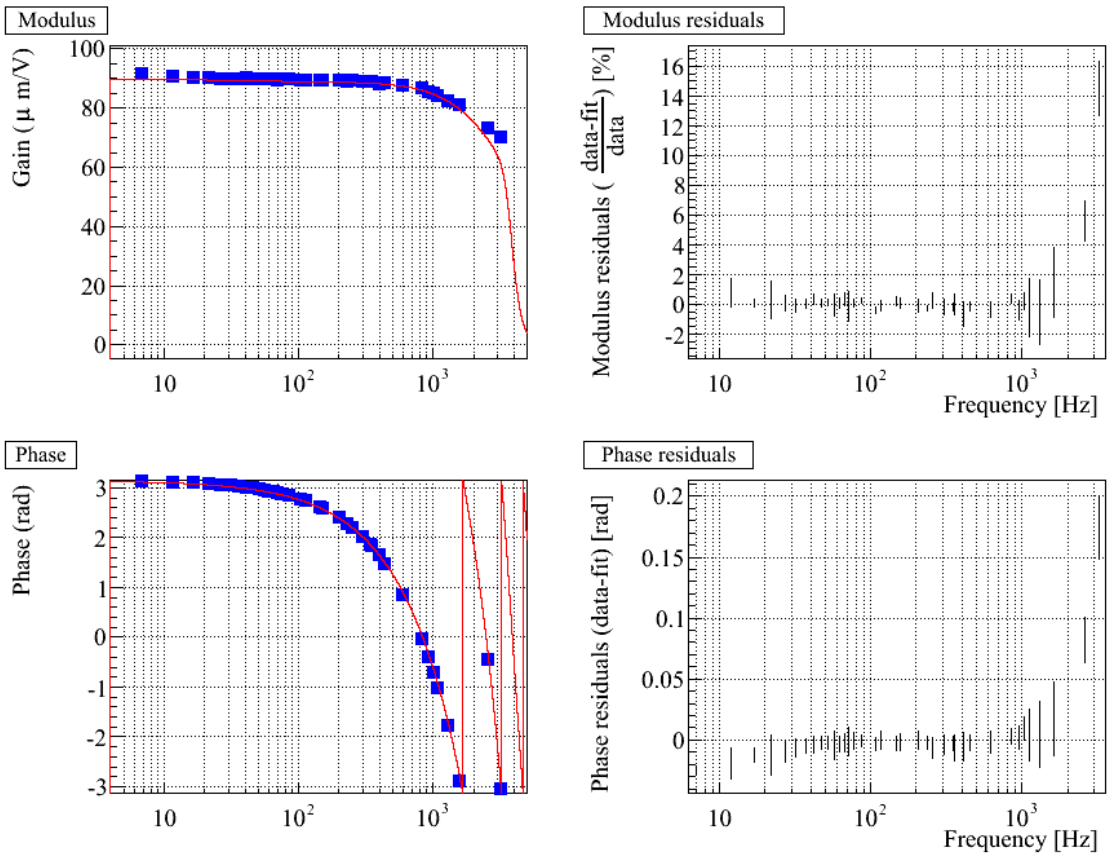

Figure 37: ***Measured actuation of the BS mirror using the four coils in LN1 mode****, fitted model and residuals.*

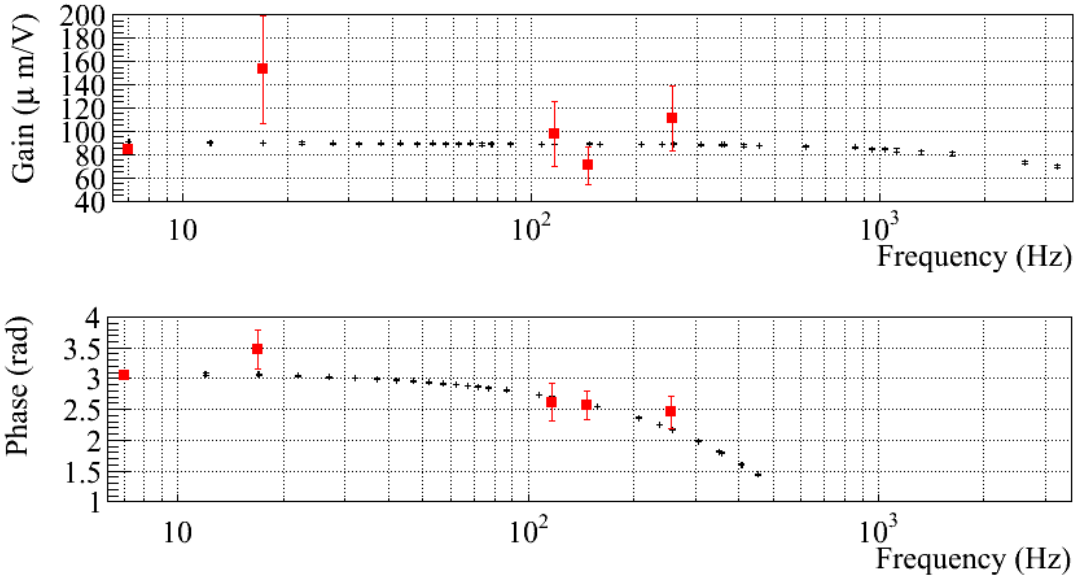

Figure 38: ***Comparison of the measurement of the actuation of the BS mirror using the four coils in LN1 mode****. Black: standard measurements. Red squares: free Michelson measurements.*

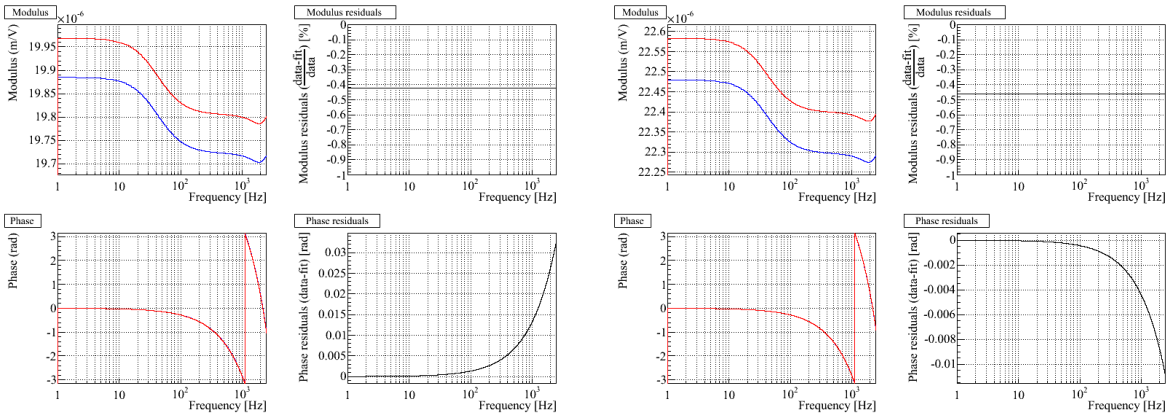

(a) WE, U-D coils, LN1

(b) NE, U-D coils, LN1

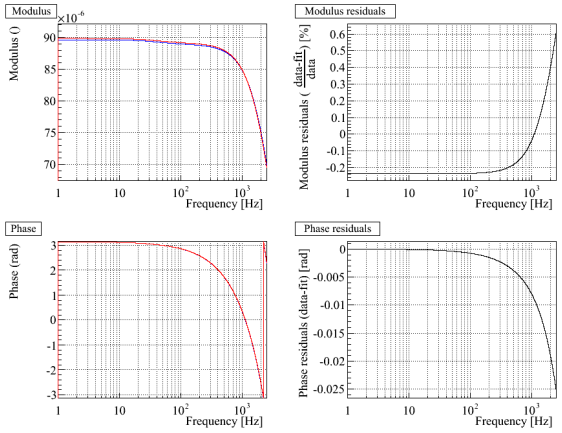

(c) BS, four coils, LN1

Figure 39: ***Comparison of the mirror actuation parameterizations used online during VSR3 with the new parameterizations.*** *For each suspension, the left plots show the comparison of the TFs: old one in red, new one in blue ; the right plots show the residuals between the models. Note that the pendulum model which is the same in both parameterizations is not shown in the TFs.*

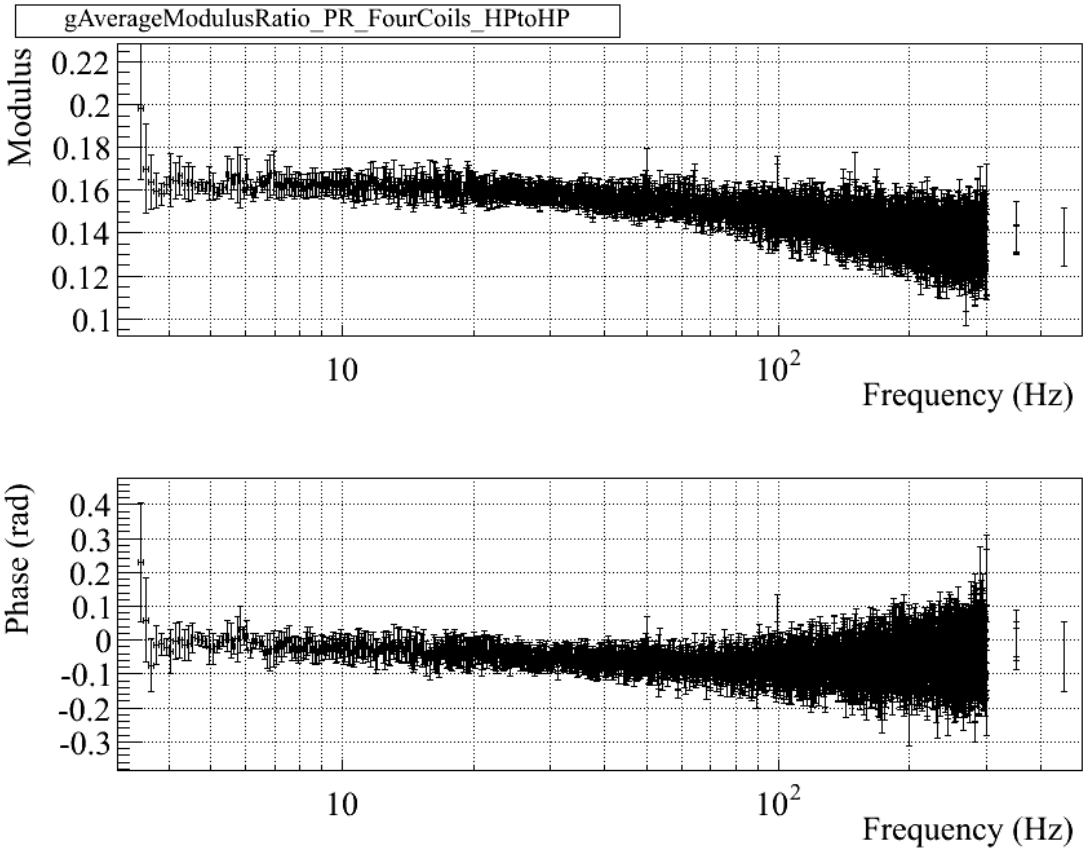

Figure 40: ***Measured ratio of the PR over BS mirror actuation response (in HP mode).***

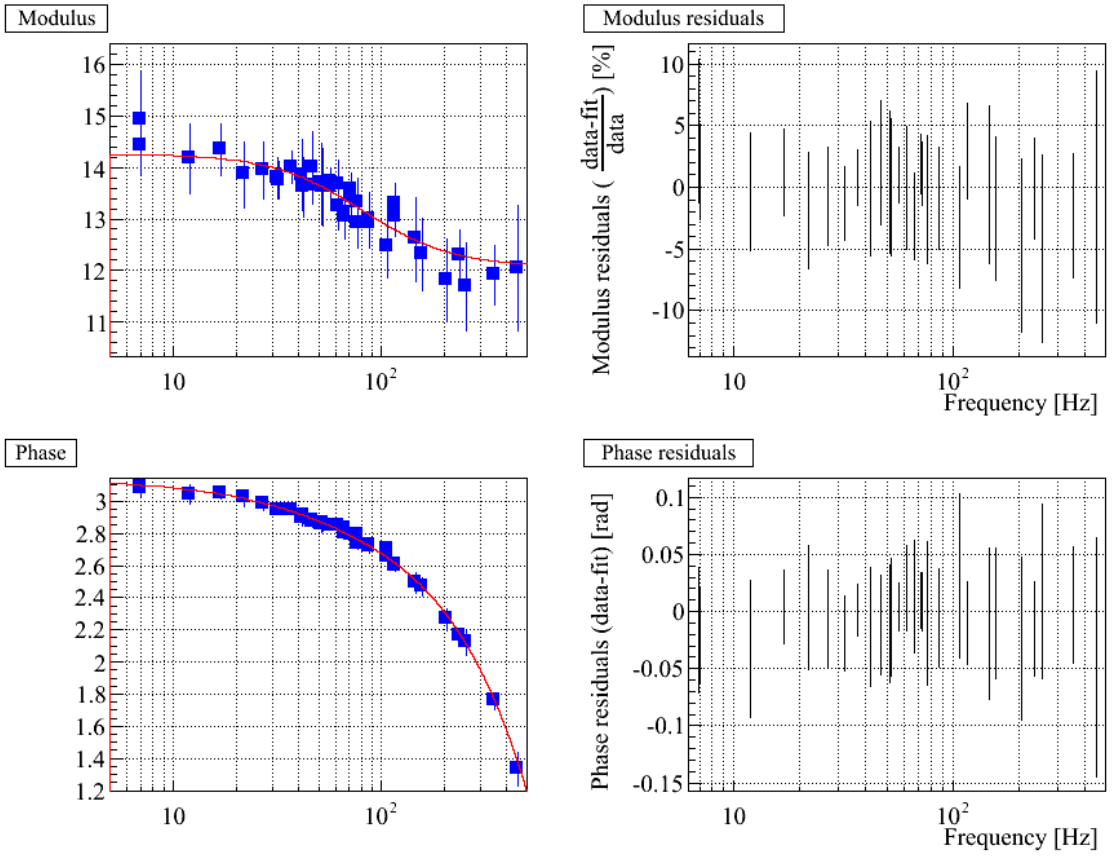

Figure 41: ***Measured actuation TF of the PR mirror actuation****, fitted model and residuals.*

4 Calibration of the marionette actuation

The marionette actuation is defined as the TF (with modulus in m/V) from the correction signal stored in the Virgo data to the induced mirror motion[5]. The time reference for the mirror motion is the GPS time.

In the plots that are shown, the actuation is corrected for a mechanical model of the pendulum[6], defined as **two** 2nd order low-pass filters with $f_0 = 0.6\,\mathrm{Hz}$ and $Q = 1000$.

4.1 Description of the measurements

The calibration of the NE (U-D coils) and WE (U-D coils) mirror actuation in LN1 mode is used as reference to measure the NE and WE marionette actuations.

An intermediate step consists in measuring the Marionette/Mirror TF ratio in step 12. This ratio is then multiplied by the model of the mirror actuation (U-D coils, in LN1 mode) to obtain the marionette actuation. Only the points where the coherence is higher than 90% have been used to estimate the TF ratio.

This analysis assumes that the ITF response (in particular the optical gain) is stable between the two datasets. In principle this is the case since both datasets are taken within 3 minutes. Such data were taken at different times and monitored during VSR3. The stability of the measurements validates this hypothesis.

The injected noise has been white noise from a few Hz to ~ 200 Hz (with few lines at low frequency). Different amplitudes of the noise were injected in order to check the linearity of the response.

4.2 Calibration of the WE and NE marionettes

The measured ratios of the WE and NE marionette to mirror responses are shown figures 45 and 47 (the mirror and marionette actuations being corrected for their pendulum mechanical model). The monitoring of these ratios as function of time are shown at some frequencies figures 42 and 44.

The obtained marionette TFs are shown figures 46 and 48 along with the fitted model and residuals. The fits were performed between 9 Hz and 200 Hz. The fit parameters are given in

[5] The marionette longitudinal actuation is done through two coils (left and right). Emphasis filters are set in the DSP for both coil channels in order to compensate for de-emphasis filters used in the coil drivers. The resistance of the coil channel is $R \sim 16.5\,\Omega$ and its inductance is $L \sim 214\,\mathrm{mH}$: the L-R circuit results in a pole $R/(2\pi L)$ around $12 - -13\,\mathrm{Hz}$.

[6] This model is not accurate. A more precise model [6] is two 2nd order low-pass filters at frequencies 0.46 Hz and 0.98 Hz, both with a quality factor of 100.

the table 6. A 2nd order low-pass filter at 1 kHz has been arbitrarily added in order to have a non-divergent TF parameterization. Below 100 Hz, the residuals are flat, lower than 3% in modulus and better than 30 mrad in phase.

Note that the 4 μs timing systematic error are negligible for the marionettes: at 100 Hz, it corresponds to less than 3 mrad phase error.

The new parameterizations are compared to the ones from note [2] in the figure 50. Between 5 Hz and 100 Hz, the parameterizations agree within 3%/200 mrad in modulus and phase respectively.

4.3 Cross-check of the marionette actuation measurements

The standard way to measure the marionette actuation is done as a combination of measurements of the actuation in HP mode, measurements of the LN1/HP ratio and measurements of the marionette/mirror ratio. In order to cross-check the results, a direct measurement of the WE and NE marionette actuations has been performed using free swinging Michelson data. Due to the limited dynamic of induced mirror motion through the marionette, only some frequencies below 6 Hz have been measured. The results are shown in figure 49. There is no clear overlap of the measurements in frequency. However, no strong offset is observed at the limit between both measurements. At 5.5 Hz, a measurement is obtained by both methods: they agree within statistical errors of 10%/10 mrad in modulus and phase respectively. No systematic error could be highlighted.

4.4 Tables

	WE	NE
Gain (μm/V)	3.859 ± 0.015	4.074 ± 0.013
Raw delay (μs)	$(1609) \pm 14)$	(672.6 ± 15)
Delay (μs)	1459.7 ± 14	523.3 ± 19
Φ_0 (rad)	0	0
Pole frequency (Hz)	15.528 ± 0.080	15.159 ± 0.058
Zero frequency (Hz)	–	406.0 ± 17
Pole frequency (Hz)	–	–
Complex zero f_0 (Hz)	192.03 ± 2.5	–
Complex zero Q	0.681 ± 0.0056	–
2nd order low-pass	$f_0 = 1000\,\mathrm{Hz}$, $Q = 0.7$	
Pendulum	**Two** 2nd order low-pass filters: $f_0 = 0.6\,\mathrm{Hz}$, $Q = 1000$	
χ^2/ndf	2310.09/2143	1647.23/1804

Table 6: ***WE and NE marionette actuation parameterizations.*** *Fit computed from 9 Hz to 200 Hz. The χ^2/ndf of the fits are given. Residuals are within 5% in modulus and 50 mrad in phase up to 150 Hz. The raw delays are the delay measured using the raw delays from the mirror actuation measurements. The delay has been corrected for the PrCa and sensing delays to take as reference the correction channels (i.e. Sc_WE_zMar): delay = raw_delay − 100 − 49.3 μs. Applying these TFs to the correction channels Sc_WE_zMar should enable to estimate the induce motion at absolute GPS time. Note that the error matrix from Minuit is not positively defined ("ERR MATRIX NOT POS-DEF") indicating that the parameter error estimation is not accurate.*

4.5 Figures

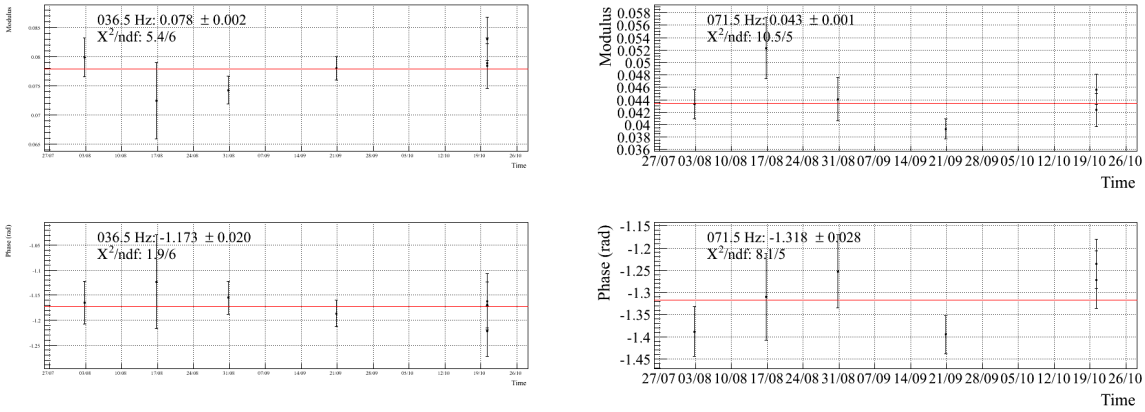

(a) 36.5 Hz

(b) 71.5 Hz

(c) 121.5 Hz

Figure 42: ***Measured WE marionette to mirror actuation (WE, U-D coils) TF ratio as function of time*** *at four different frequencies. The mirror and marionette actuations have been corrected for their pendulum mechanical models.*

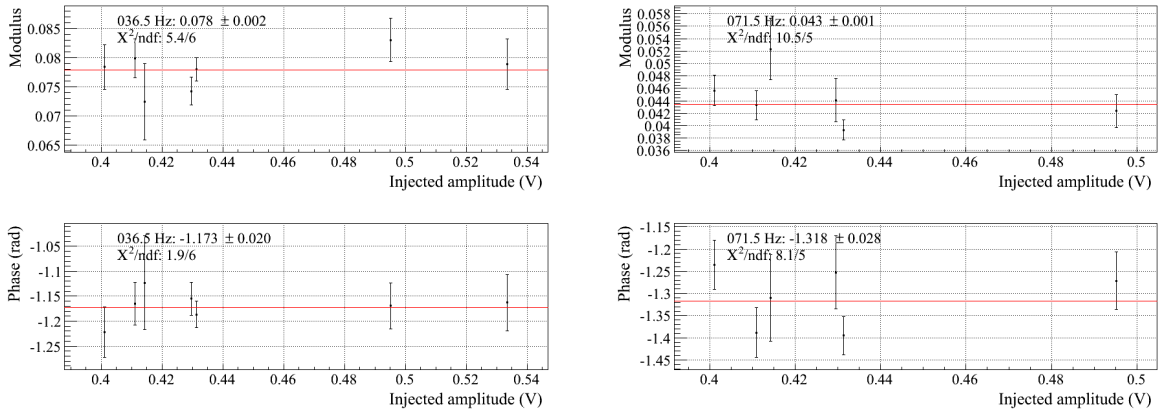

(a) 36.5 Hz

(b) 71.5 Hz

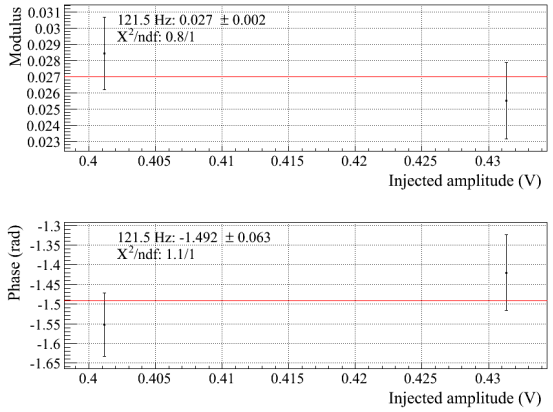

(c) 121.5 Hz

Figure 43: ***Measured WE marionette to mirror actuation (WE, U-D coils) TF ratio as function of amplitude of injected noise*** *at four different frequencies. The mirror and marionette actuations have been corrected for their pendulum mechanical models.*

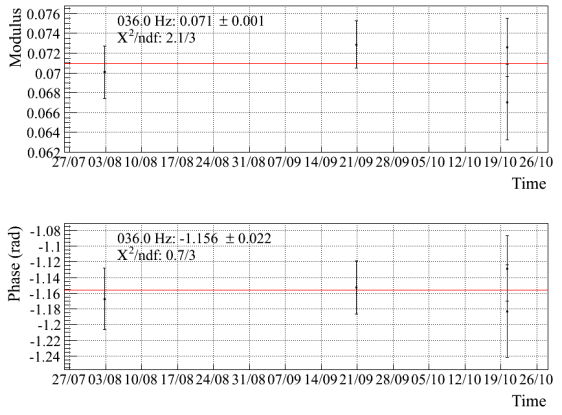

(a) 36.0 Hz

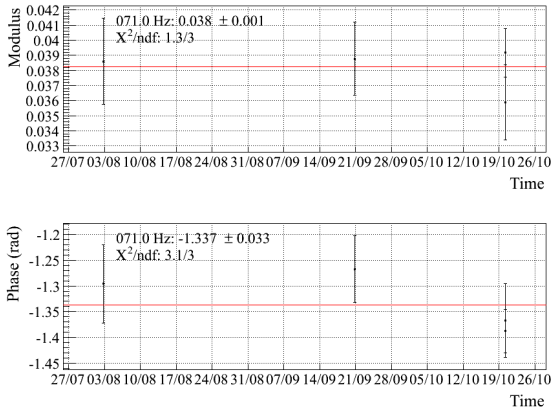

(b) 71.0 Hz

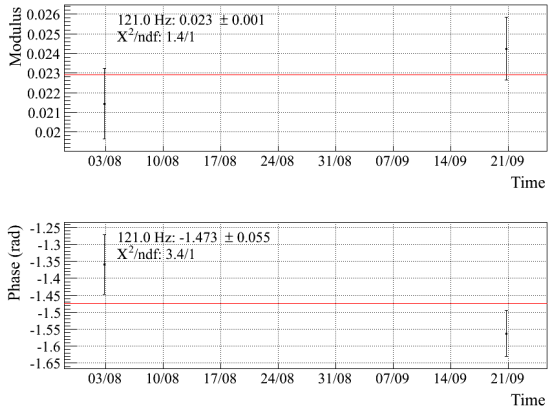

(c) 121.0 Hz

Figure 44: ***Measured NE marionette to mirror actuation (NE, U-D coils) TF ratio as function of time*** *at four different frequencies. The mirror and marionette actuations have been corrected for their pendulum mechanical models.*

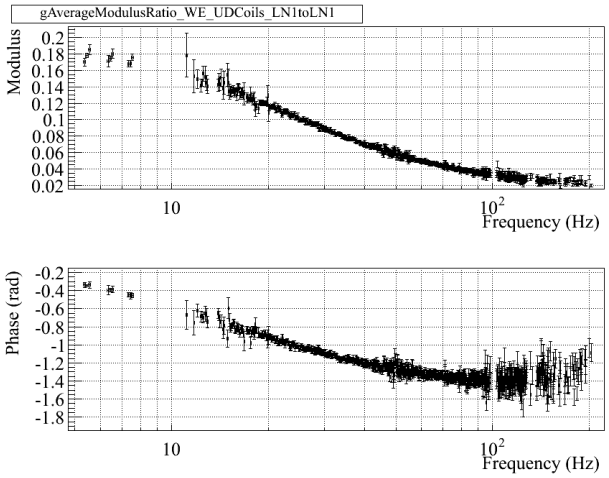

Figure 45: ***Averaged marionette to mirror actuation TF ratio of the WE suspension.*** *The mirror and marionette actuations have been corrected for their pendulum mechanical models.*

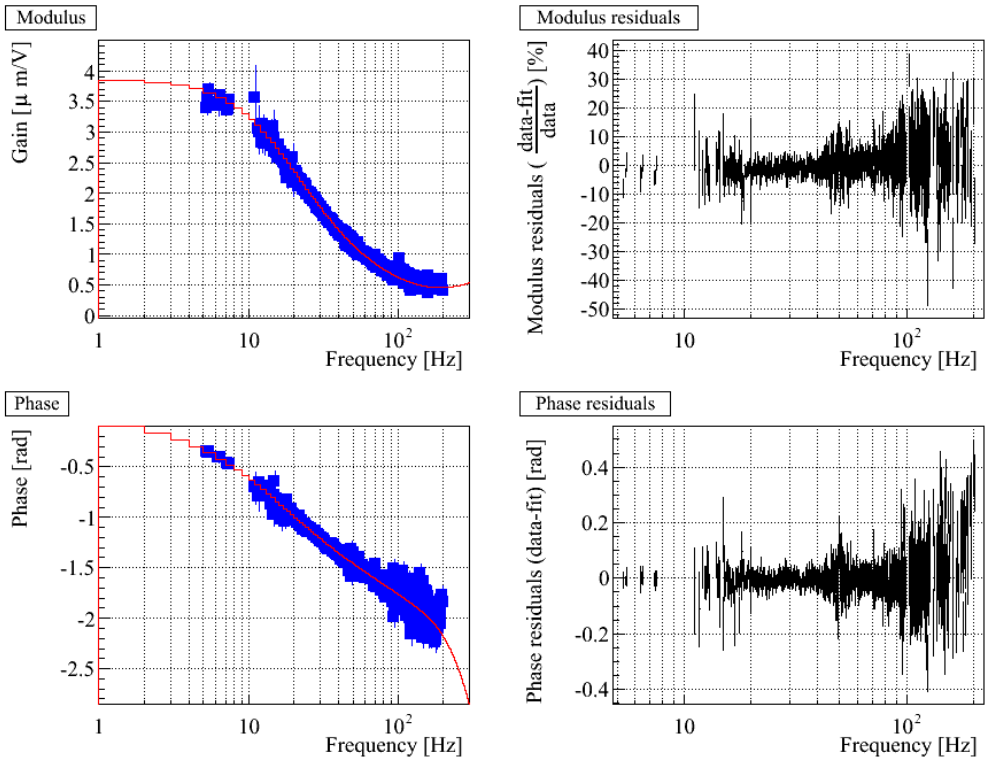

Figure 46: ***Measured WE marionette actuation TF****, fit and residuals.*

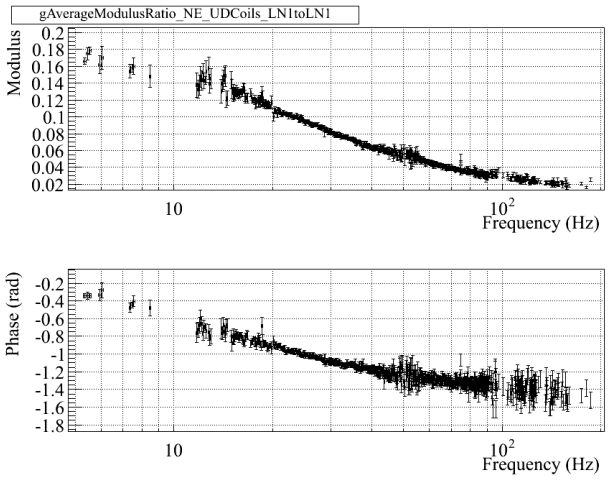

Figure 47: ***Averaged marionette to mirror actuation TF ratio of the NE suspension.***

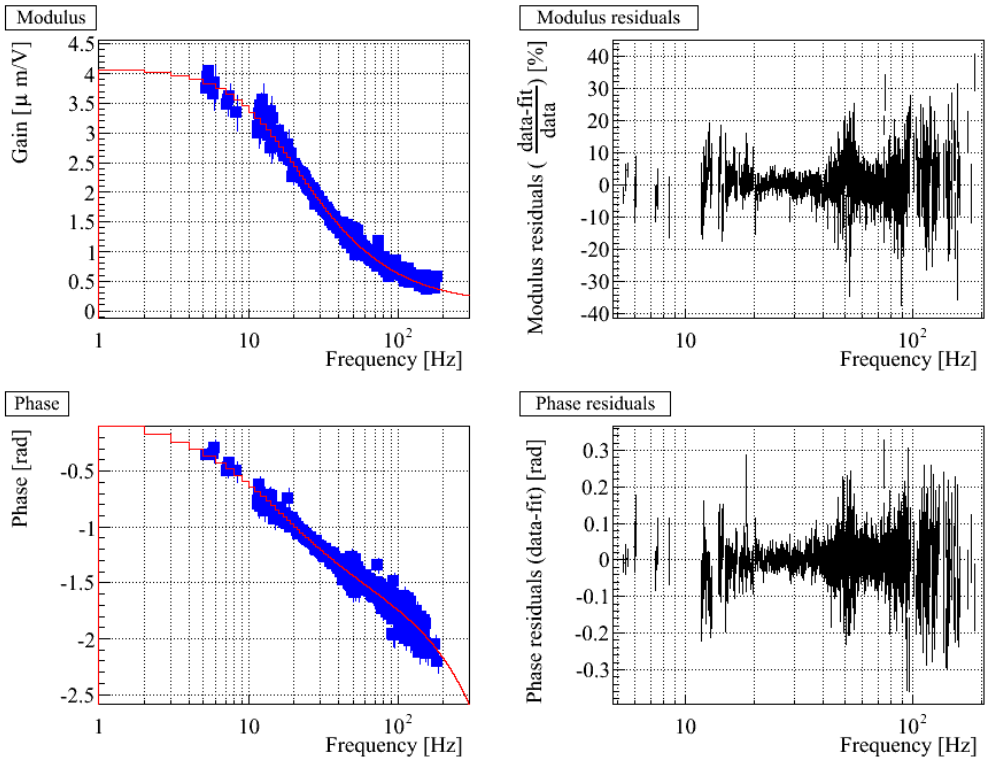

Figure 48: ***Measured NE marionette actuation TF****, fit and residuals.*

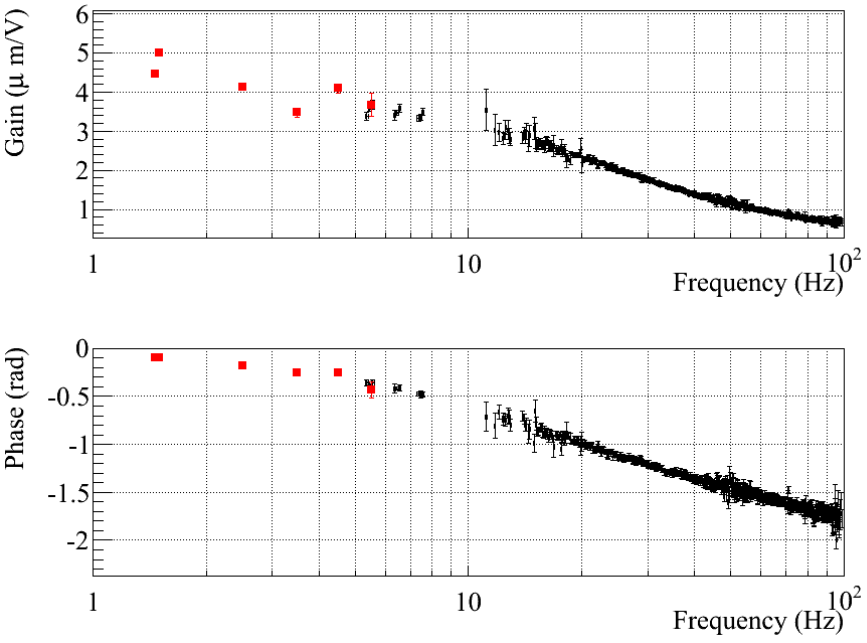

(a) WE marionette

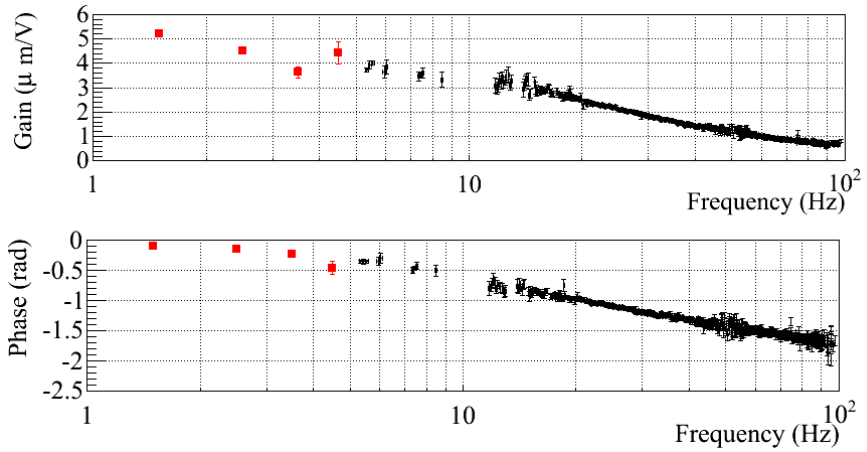

(b) NE marionette

Figure 49: ***Comparison of the marionette actuation measurements.*** *Black (above 5 Hz): standard measurements. Red (below 5 Hz): free Michelson measurements.*

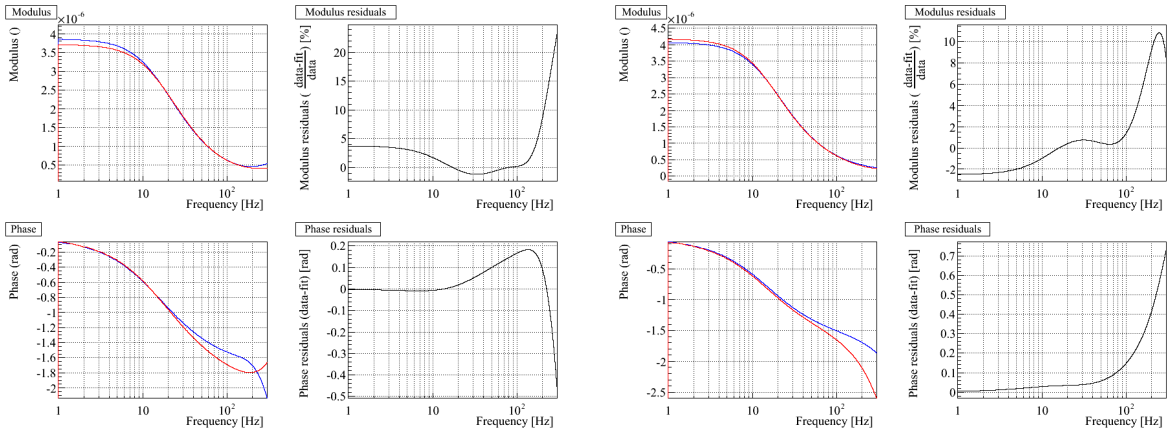

(a) WE, Marionette

(b) NE, Marionette

Figure 50: ***Comparison of the models from note [2] (red, corrected for factor 1.33) with the new models (blue)*** *For each comparison, the left plots show the comparison of the TFs: old one in red, new one in blue; the right plots show the residuals between the models. Note that the fixed 2nd order low-pass filter and pendulum model which are the same in both parameterizations are not shown in the TFs.*

5 VSR3 hardware injection models

Hardware injections (HI) of fake gravitationnal wave signals have been performed during VSR3 through the WE mirror actuation through the L-R coils in LN1 mode. The HI process takes as input the $h(t)$ signal to be injected in the ITF and computes the excitation signal to be sent to the WE mirror actuation (Ca_WE_zMirLR). This conversion is done using the inverse TF of the mirror actuation response.

Two different parameterizations for the actuation response have been used during VSR3, before and after September 3rd 2010, around 14h45 UTC (see logbook entry 27701):

- before: parameterizations from pre-run calibration (note [2]).
- after: the actuation gain has been increased by a factor 1.33 to take into account a change of gain in the DSPs.

The actuation parameters used online are given in the table 7. The TFs used after September 3rd 2010 are compared to the final parameterization from this note (see table 4) in figures 51 and 52. Differences are lower than 1.2% in amplitude and 10 mrad/1 μs in phase/timing from 10 Hz to 2 kHz.

Before September 3rd 2010, the injected signals were louder (too loud) by a factor 1.33 in amplitude.

		Up to 03/09/2010	From 03/09/2010
WE, LR	Gain (μm/V) Delay (μs) Φ_0 (rad)	15.16 650.6 π	20.16 650.6 π
h	Pendulum	Low-pass frequency: 0.6 Hz Quality factor: 1000	Low-pass frequency: 0.6 Hz Quality factor: 1000
NE, LR	Gain (μm/V) Delay (μs) Φ_0 (rad)	17.06 645.0 π	22.73 645.0 π
	Pendulum	Low-pass frequency: 0.6 Hz Quality factor: 1000	Low-pass frequency: 0.6 Hz Quality factor: 1000

Table 7: ***WE (L-R coils) and NE (L-R coils) mirror actuation parameterizations used for the hardware injections during VSR3****. The sign of the injections were checked before the start of VSR3: it resulted in the use of a phase of π in the TFs.*

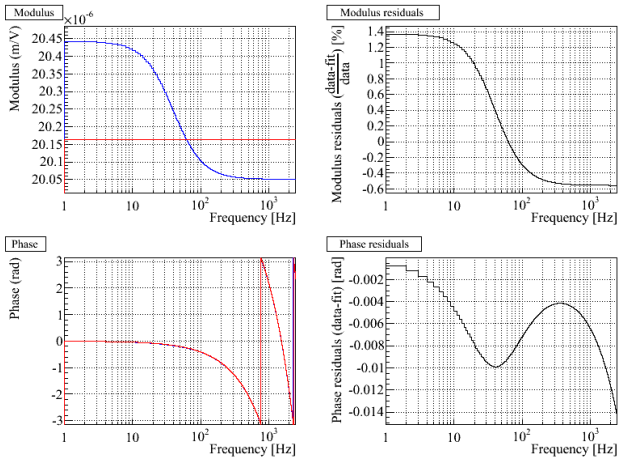

(a) September 3rd to October 2010

Figure 51: ***Actuation models used for the hardware injections during VSR3 (red, after Sept. 3rd) and from this note (blue). Right: residuals ;*** *Modulus:* $(G_{HImodel} - G_{CurrentModel})/G_{HIModel}$ *; Phase:* $\Phi_{HImodel} - \Phi_{CurrentModel}$*. Actuation of the WE mirror using the L-R coils, in LN1 mode.*

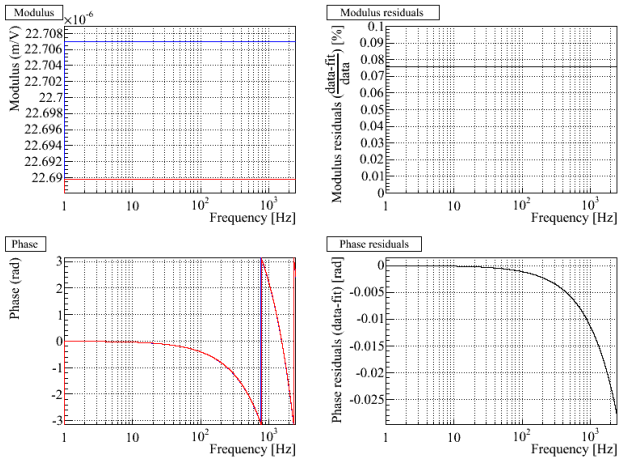

(a) September 3rd to October 2010

Figure 52: ***Actuation models used for the blind hardware injections during VSR3 (red, after Sept. 3rd) and from this note (blue). Right: residuals ;*** *Modulus:* $(G_{HImodel} - G_{CurrentModel})/G_{HImodel}$ *; Phase:* $\Phi_{HImodel} - \Phi_{CurrentModel}$*. Actuation of the NE mirror using the L-R coils, in LN1 mode.*

6 Conclusions

The full VSR3 calibration has been computed with data from July 2010 to October 2010, including pre- and post-run measurements and run periodic measurements.

The **dark fringe readout** has been calibrated (see note [5]), the timing being related to the absolute GPS time. The timing has been computed from the time series stored in FrVect setting the value of sample i at the time $startX[0] + i \times dx[0]$. The 20 kHz dark fringe channel models, given in the table 1, are **understood from 1 Hz to 10 kHz within systematic errors of** ± 4 μs**.** The time stability of the sensing response during VSR3 has been checked within 0.1 μs.

The **BS, WE and NE mirror actuations in LN1 mode have been measured from 5 Hz to ∼1 kHz**. The monitoring data repeated every week or two weeks during VSR3 have permitted to find during the run that the gain of the end mirror actuation had been changed and to correct the parameterizations used online. Except for this change, the monitoring data have shown that the parameters have been stable within statistical errors from July to October 2010. The parameterizations are given in the tables 3 for the controls and 4 for the hardware injections. The delays are related to the absolute GPS time. Up to 1 kHz, the statistical errors are of the order of 1%/10 mrad in modulus and phase respectively at the frequencies that where monitored during the run.

The following table gives a summary of the statistical and systematic errors on the NE, WE and BS mirror actuation in LN1 mode between 5 Hz and 1 kHz. The systematic errors are dominated by errors coming from the LN1/HP measurements: some coils show few percents dependence of the modulus ratio on the injected noise amplitude.

		Modulus	Phase
stat.	HP	1%	10 mrad
	LN1/HP	0.3%	3 mrad
syst.	HP	–	–
	LN1/HP	3%	3 μs
	Sensing timing	–	1 μs
	Absolute timing	–	4 μs

The **PR mirror actuation response** has been measured below 300 Hz after the run. The parameterization is given in the table 5. **Up to 300 Hz, the statistical errors and residuals are within 5%/50 mrad in modulus and phase respectively.** Systematic errors are expected to be negligible.

The **marionette actuation responses have been measured from 5 Hz to ∼300 Hz.** The parameterizations are given in the table 6 for WE and NE. The delays are related to the absolute GPS time. The monitoring data during VSR3 and the different injected amplitudes

did not show any variations within statistics of the order of 3% and 30 mrad. **The systematic errors include the errors from the mirror actuation – ∼3% in modulus** and negligible in phase.

References

[1] T. Accadia et al (Vigo collaboration) *Calibration and sensitivity of the Virgo detector during its second science run* submitted to CQG, arXiv:1009.5190v1.

[2] L. Rolland *Preliminary VSR3 calibration (July 2010)* (2010) VIR-0477A-10.

[3] L. Rolland *Stability of the timing system during VSR2* (2010) VIR-0354A-10.

[4] L. Rolland *VSR2 mirror and marionette actuator calibration* (2010) VIR-0076B-10.

[5] L. Rolland *Calibration status in September 2009* (2009) VIR-076A-09.

[6] D. Huet, *Actuation noise projection for Virgo+MS* (2009) VIR-0573A-09.